Correspondence to:
C. Cai,
chenxia.cai@arb.ca.gov

Simulating the Weekly Cycle of NO_x-VOC-HO_x-O_3 Photochemical System in the South Coast of California During CalNex-2010 Campaign

Chenxia Cai[1], Jeremy Avise[1,2], Ajith Kaduwela[1,3], John DaMassa[1], Carsten Warneke[4,5], Jessica B. Gilman[5], William Kuster[5], Joost de Gouw[4,6], Rainer Volkamer[4,6], Philip Stevens[7], Barry Lefer[8,9], John S. Holloway[4,5], Ilana B. Pollack[4,5,10], Thomas Ryerson[5], Elliot Atlas[11], Donald Blake[12], Bernhard Rappenglueck[8], Steven S. Brown[5], and William P. Dube[4,5]

[1]California Air Resources Board, Sacramento, CA, USA, [2]Laboratory for Atmospheric Research, Washington State University, Pullman, WA, USA, [3]Air Quality Research Center, University of California, Davis, CA, USA, [4]Cooperative Institute for Research in Environmental Sciences, University of Colorado Boulder, Boulder, CO, USA, [5]Chemical Sciences Division, Earth System Research Laboratory, National Oceanic and Atmospheric Administration, Boulder, CO, USA, [6]Department of Chemistry and Biochemistry, University of Colorado Boulder, Boulder, CO, USA, [7]School of Public and Environmental Affairs and Department of Chemistry, Indiana University, Bloomington, IN, USA, [8]Department of Earth and Atmospheric Sciences, University of Houston, Houston, TX, USA, [9]Now at Earth Science Division, National Aeronautics and Space Administration, Washington, DC, USA, [10]Now at Department of Atmospheric Science, Colorado State University, Fort Collins, CO, USA, [11]Division of Marine and Atmospheric Chemistry, Rosenstiel School of Marine and Atmospheric Science, University of Miami, Miami, FL, USA, [12]School of Physical Sciences, University of California, Irvine, CA, USA

Abstract United States Environmental Protection Agency guidance on the use of photochemical models for assessing the efficacy of an emissions control strategy for ozone requires that modeling be used in a relative sense. Consequently, testing a modeling system's ability to predict changes in ozone resulting from emission changes is critical. We evaluate model simulations for precursor species (NO_x, CO, and volatile organic compounds [VOCs]), radicals (OH and HO_2), a secondary pollutant (O_3), and the model response of these compounds to weekend/weekday emission changes during California Nexus study in 2010. The modeling system correctly simulated the broad spatial and temporal variation of NO_x and O_3 in California South Coast. Although the model generally underpredicted the daytime mixing ratios of NO_2 at the surface and overpredicted the NO_2 column, the simulated weekend to weekday ratios are consistent with each other and match the observed ratios well. The modeling system exhibited reasonable performance in simulating the VOC compounds with fossil fuel origins but has larger bias in simulating certain species associated with noncombustion sources. The modeling system successfully captured the weekend changes of the enhancement ratios for various VOC species to CO and the relative changes of HO_x, which are indicators of faster chemical processing on weekends. This work demonstrates satisfactory model performances for O_3 and most relevant chemical compounds with more robust performance in simulating weekend versus weekday changes. Improved planetary boundary layer height simulations, a better understanding of OH-HO_2 cycling, continued improvement of emissions, especially urban biogenic emissions and emissions of oxygenated VOCs, are important for future model improvement.

1. Introduction

It is well known that exposure to tropospheric ozone (O_3) is harmful to human beings, vegetation, and ecosystems. The Clean Air Act requires the United States Environmental Protection Agency (United States EPA) to set national ambient air quality standards for O_3 to provide adequate protection to human health and the environment. Tropospheric O_3 is formed through a complex series of photochemical reactions involving volatile organic compounds (VOCs) and nitrogen oxide (NO_x = NO + NO_2) in the presence of sunlight. Due to the nonlinear nature of the photochemistry, a reduction in emissions of VOCs or NO_x may lead to an increase, decrease, or no-change in ambient O_3 concentration, depending on the relative levels of VOCs and NO_x (Finlayson-Pitts & Pitts, 1986; Seinfeld & Pandis, 2006). O_3 formation is also sensitive to other factors such as the species that comprise the ambient VOC mixture and environmental conditions (Stephens

et al., 2008). Many studies have shown that in areas of high NO_x emissions, O_3 concentration can exhibit a day-of-week dependence, with peaks occurring during the weekend despite lower NO_x emissions on those days (Altshuler et al., 1995; Austin & Tran, 1999; Cleveland et al., 1974; Elkus & Wilson, 1977; Horie et al., 1979; Levitt & Chock, 1976; Murphy et al., 2007). This phenomenon has become known as the O_3 weekend effect. In the South Coast Air Basin (SoCAB) of California, a region with historically severe air quality issues, the O_3 weekend effect has been studied extensively (Baidar et al., 2015; Blanchard & Tanenbaum, 2003; Chinkin et al., 2003; Fujita et al., 2003; Kim et al, 2016; Heuss et al., 2003; Marr & Harley, 2002; Pollack et al., 2012; Qin et al., 2004; Warneke et al., 2013; Yarwood et al., 2003). The general consensus is that in NO_x-saturated areas such as SoCAB the O_3 weekend effect results from two processes: (1) reduced O_3 loss by titration due a decrease in NO_x emissions as a result of fewer diesel trucks on the road during the weekend and (2) enhanced ozone production due to faster photochemical processing at lower NO_x mixing ratios.

The California Research at the Nexus of Air Quality and Climate Change (CalNex) field campaign was conducted throughout California during the months of May–July 2010 to address atmospheric chemistry in the region, as well as the interactions between air quality and climate change. This field campaign acquired a wealth of ambient measurements including O_3, particular matter, and precursor species including NO_x and speciated VOCs as well as intermediate chemical species. Analysis of the measurements from the CalNex field campaign by Pollack et al. (2012) showed that on the weekend in SoCAB, photochemical processing was faster and ozone production efficiency was greater compared to weekdays. As a result of this faster photochemical processing, ambient mixing ratios for short-lived VOCs also exhibited a weekly cycle (Warneke et al., 2013). Combining CalNex observations with long-term O_3 data from routine ground monitoring measurements, Baidar et al. (2015) reported that despite the continued widespread existence of an O_3 weekend effect, the likelihood of higher O_3 on any given weekend in SoCAB has decreased in recent years, with the lowest probability of occurrences in the eastern SoCAB. Measurements from CalNex field campaign have also been applied in performance evaluation of various modeling studies (e.g. Angevine et al., 2012; Baker et al., 2013; Baker et al., 2015; Chen et al., 2013; Ensberg et al., 2013; Fast et al., 2014; Kelly et al., 2014; Kim et al., 2016; Huang et al., 2014; Woody et al., 2016).

Three-dimensional photochemical transport models are mathematical representations of the state-of-the-science in our understanding of the physical and chemical processes in the atmosphere and have been a useful tool for studying the weekend O_3 effect. For example, photochemical models were used to quantify the impact of changes in the magnitude and timing of on-road mobile emissions, from weekday to weekend, on the formation of ozone in central (Marr & Harley, 2002) and Southern (Yarwood et al., 2003) California. These studies found that the overall reduction in NO_x emissions on weekends was the dominant factor driving the weekend O_3 effect, while emission carryover from Friday and Saturday night traffic, different timing of weekend emissions, and carryover of pollution aloft were not significant factors. Kim et al. (2016) developed a fuel-based inventory for vehicle emissions of NO_x and CO for Southern California. The model simulation in that study was also used to demonstrate that a decrease in NO_x emissions on weekends resulted in enhanced photochemistry and an increase in O_3 and O_x ($O_3 + NO_2$). In general, past modeling studies on the weekend O_3 effect have mostly focused on the changes of O_3 and NO_x but rarely investigated the associated changes in VOCs and radical species.

In addition to investigate observed phenomena such as the weekend O_3 effect, photochemical models have been widely used as reliable quantitative tools in developing emission control strategies for the attainment of ozone and particulate matter standards. United States EPA guidance for photochemical modeling requires that model results be used in a relative rather than absolute sense for regulatory applications (United States Environmental Protection Agency, 2018). As such, effective models must not only predict secondary pollutants, associate precursor species, and the key intermediate constituents but also the response of these chemical compounds to changes in emissions. The day-of-week variation in NO_x and VOC emissions (i.e., weekend vs weekday) provides a real-world test to evaluate the model's capability in simulating the response of different chemical compounds to emission changes.

In this work, we present an evaluation of fine-resolution 3-D regional air quality model simulations over California for O_3, NO_x, individual VOC species, and HO_x (OH and HO_2) using colocated measurements of chemical compounds from the CalNex 2010 field campaign as well as measurements from the routine

ground monitoring stations. Particular emphasis is placed on the model's capability in capturing the weekend versus weekday changes of these chemical compounds in the SoCAB from May to July 2010 using California Air Resources Board's (CARB) latest 2010 emission inventories that incorporate day-of-the-week emission changes. Following the introduction, we describe the model configuration and observational data used in the model evaluation in section 2. We compare the NO_x and VOC emissions on weekdays and weekends in section 3 and the evaluate model outputs with observations from different measurement platforms in section 4. Key findings from this work are summarized and discussed in section 5.

2. Methods

2.1. Model Configuration

Air quality model simulations over California from 1 May to 31 July 2010 were conducted using the Community Multiscale Air Quality (CMAQ v5.02) regional photochemical model (Appel et al., 2013). CMAQ was driven by meteorological inputs from simulations with the Weather Research and Forecasting (WRF v3.4) model (Skamarock et al., 2008) and the 2010 California emission inventory from CARB. Among the mechanism options used were the SAPRC07 toxic version (SAPRC07TC) for gas phase chemistry and AERO6 for aerosol representation in CMAQ. Inline photolysis rate calculations were used to update the photolysis rates based on the simulated levels of cloud cover, aerosols, and ozone in the atmosphere. The CMAQ model was applied using a 4×4 km^2 horizontal grid resolution. The vertical grid structure includes 30 vertical layers from ground level to 100 mb with the highest resolution below 5 km. The model domain, shown in Figure S1 in the supporting information, covers all of California, Nevada, and part of the Pacific Ocean to the west. Chemical boundary conditions were developed by mapping 6-hr output (interpolated to 1-hr data) from the Model for Ozone and Related chemical Tracers, version 4 (MOZART-4) global chemical transport model driven by Goddard Earth Observing System Model, version 5 meteorological fields (Emmons et al., 2010; http://www.acom.ucar.edu/wrf-chem/mozart.shtml) onto the CMAQ model domain and mapping the MOZART-4 chemical species to the SAPRC07T mechanism. While the model domain covers California, this study focuses on SoCAB, for which the boundary is marked with a solid black line in Figure S1 in supporting information.

In the WRFv3.4 model simulation three nested domains with horizontal grid sizes of 36×36, 12×12, and 4×4 km^2 were employed to adequately resolve synoptic-scale flow, as well as the fine-scale flow (e.g., landsea breeze, mountain-valley wind, and local eddies) induced by the complex terrain over California. Results from the innermost 4×4 km^2 domain, which is consistent with the CMAQ domain, were used as meteorological input for the CMAQ model simulations. North American Regional Reanalysis (NARR) data were used to provide initial and boundary conditions for WRF. Physics schemes employed in the WRF simulation were WRF single moment 6-class microphysics scheme, Rapid Radiative Transfer Model long-wave radiation scheme, Dudhia short-wave radiation scheme, Yonsei University planetary boundary layer (PBL) scheme, Pleim-Xiu land surface model, Kain-Fritsch cumulus scheme (only applied to the 36×36 and 12×12 km^2 outer domains), and topographic surface wind correction on the innermost domain (Jimenez & Dudhia, 2012). Sea surface temperature was updated with Global Ocean Data Assimilation Experiment sea surface temperature every 6 hr for all the three domains during the simulation. Four-dimensional data assimilation was applied to the outermost domain to nudge simulation results to the driving NARR reanalysis fields. WRF was reinitialized to the NARR reanalysis fields every 6 days. For each 6-day simulation, the first day simulation was discarded as model spin-up. MCIPv4.1 was used to generate CMAQ ready meteorology inputs from the WRF simulations. WRF output for temperature, relative humidity, wind speed, and wind direction were evaluated against the available observation data at 29 monitoring sites in SoCAB from May to July 2010. Statistical metrics for model performance including mean bias, normalized mean bias, normalized mean error and root-mean-square error are shown in Table S1 for all days, weekdays only, and weekends only. WRF model performance is consistent with other WRF simulations for CalNex 2010 (Baker et al., 2013; Fast et al., 2014), and there are no major performance differences between weekdays and weekends.

The latest 2010 emissions inventory developed by the CARB for CalNex was used in this work. Emissions from all major source categories including area, point, mobile, biogenic, road dust, and ocean-going vessel emissions were represented with day-specific adjustments whenever possible to reflect the day-of-the-

Table 1
Summary of Measured Chemical Species and the Instrument Techniques During CalNex Field Campaign

Species	Technique	Sample interval	Reference
CalNex Pasadena Supersite			
O_3	UV differential absorption (Thermo 49c)	1 min	
NO	Chemiluminescent (Thermo 42i-TL)	1 min	
NO_2	LED-CE_DOAS	1 min	
CO	Vacuum UV resonance fluorescence (AeroLaser AL 5001)	1 min	Gerbig et al. (1999)
HCHO	Fluorometrix hantzsch reaction (AeroLaser AL 4021)	1 min	Rappenglück et al. (2010)
VOCs	GC–MS	30 min	Gilman et al. (2010)
OH	Fluorescent Assay by Gas Expansion	15 min	Dusanter et al. (2009)
CalNex P-3 Aircraft			
O_3, NO	NO/O3 Chemiluminescent	1 s	Ryerson et al. (1998)
NO_2	UV-LED photolytic conversion to NO followed by Chemiluminescent	1 s	Pollack et al. (2011)
O_3, NO, NO_2	Cavity ring-down spectroscopy	1 s	Wagner et al. (2011)
CO	Vacuum UV resonance fluorescence	1 s	Holloway et al. (2000)
VOCs	PTR-MS	1 s every 17 s	de Gouw and Warneke (2007)
VOCs	Whole air sampler	3–8 s	Colman et al. (2001), Schauffler et al. (1999)
CalNex Twin Otter Aircraft			
NO_2 Column	AMAX-DOAS	2 s	Oetjen et al. (2013)

week variability. Area and point sources were available as representations of weekday and weekend emissions for each month. Biogenic emissions were derived using the Model of Emissions and Gases and Aerosols from Nature v2.04 (Guenther et al., 2006) with updated emission factor and plant functional type data developed at the CARB (Scott & Benjamin, 2003) and MODIS 8-day Leaf Area Index data for 2010 (https://lpdaac.usgs.gov/dataset_discovery/modis/modis_products_table/mcd15a2h_v006). During our initial model performance evaluation, we found large underestimation of isoprene mixing ratios compared to ground-based urban sites in SoCAB, such as the Pasadena supersite, while the model results compare reasonably well with observations in regions where the surrounding biogenic sources are predominantly from natural ecosystems rather than urban environments (e.g., the Bakersfield supersite). This model behavior is similar to what was reported in Knote et al. (2014), where the authors applied a factor of 2.5 to all biogenic emissions in grid cells with an *urban* land use classification. Following Knote et al. (2014), in this work we applied a factor of 2.5 to isoprene and α-pinene emissions in urban grid cells.

2.2. Observation

During the CalNex-2010 field campaign, extensive airborne measurements were acquired from two ground supersites one in Pasadena (Southern California) and one in Bakersfield (central Valley), as well as through multiple mobile platforms (Ryerson et al., 2013). In this work, we utilize the measurements for O_3, NO, NO_2, CO, individual VOC, and HO_x obtained from the Pasadena supersite. For our analysis, the measurements from the Pasadena supersite were averaged to hourly data in order to compare to the hourly model output. In addition to the ground measurements at the Pasadena supersite, we also utilize data collected by the National Oceanic and Atmospheric Administration (NOAA) P-3 aircraft for six weekdays and four weekend days. For O_3, NO, and NO_2 measurements from the P-3, we primarily use the measurements from gas-phase chemiluminescence technique and substitute the missing data with the measurements from cavity ring-down spectroscopy technique. In situ measurements of VOCs were made using proton-transfer-reaction mass spectrometer (PTR-MS) on the NOAA P-3 aircraft. VOC data were also acquired using whole air sampler (WAS) canisters with postflight analysis by gas chromatography. Data from PTR-MS measurements were used for the analysis of formaldehyde, acetaldehyde, toluene, benzene, methanol, acetone, and isoprene, while data from WAS canister samplers were used for the analysis of other VOC compounds including 124-trimethyle benzene, m-xylene, o-xylene, p-xylene, propene, ethene, ethanol, acetylene, and alpha-pinene. For all the P3 measurements, we used the 1-s merged observation data and then averaged the consecutive 1-s data that fell within the same model grids. Furthermore, we also study the NO_2
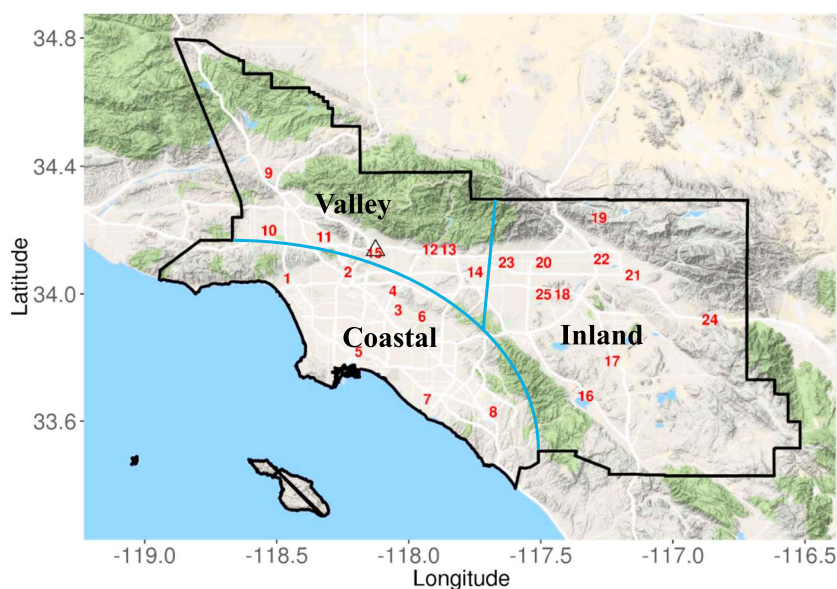
Figure 1. Map of SoCAB and the locations of Pasadena supersite (black triangle) and 25 routine ground sites. Details about each route ground sites are listed in Table S2. SoCAB = South Coast Air Basin.

column data collected by Airborne Multi-Axis Differential Optical Absorption Spectroscopy (AMAX-DOAS) instrument flying on board a NOAA Twin Otter aircraft (Oetjen et al., 2013). Detailed information about the observed chemical species and the associated measurement techniques are listed in Table 1.

Measurements of O_3, NO, NO_2, and CO from CARB's routine ground monitoring network in SoCAB are also used in this work. The observation data for these species are available from CARB's Air Quality and Meteorological Information System database (http://www.arb.ca.gov/aqmis2/aqmis2.php). The locations of monitoring sites are shown in Figure 1 as numbers, and the details about each monitoring site is listed in Table S2 in the supporting information. These sites are grouped into three subregions based on geography and proximity to the urban core emission source region, which will be used for summarizing model results: (1) coastal (source region), (2) valley (near downwind to the north), and (3) inland (far downwind to the east). Pollutant concentrations in the SoCAB vary significantly with location. While a large fraction of the primary emissions occur in the western coastal region, the highest surface ozone concentrations are usually detected in the eastern inland region.

3. Weekend Effect in the Anthropogenic Emissions of Precursor Species: NO_x, VOCs, and CO

Weekly variation of O_3 mixing ratios is mainly a result of emission changes in precursor species resulting from differences in human activities during weekdays and weekends. Figure 2 shows the integrated weekday and weekend emissions of NO_x, VOCs, and CO from different anthropogenic source categories: area, point, and on-road mobile from May to July 2010 in SoCAB. We further separated the on-road mobile emissions into diesel sources and gasoline sources that are shown as mobileD and mobileG, respectively, in Figure 2. Detailed off-road mobile emissions are considered as area sources. The dominant source of CO in the SoCAB is on-road gasoline mobile emissions, which is about 10% less on weekends compared to week-days. The second largest emission source of CO is area sources that include off-road mobile, and increases by about 45% on weekends compared to weekdays, mainly due to the increased use of off-road equipment and recreational boats on weekends. The contribution from diesel vehicles and point sources to the total CO emissions is small. Overall, the CO anthropogenic emissions in SoCAB are 4% higher on weekends compared to weekdays. Compared to CO, emissions of NO_x show much larger variation from weekday to weekend. On-road mobile emissions from diesel vehicles are the primary source of NO_x during weekdays, and this source decreased by about 50% on weekends, making mobile gasoline and area emissions the two largest sources on weekends. Emissions of NO_x from gasoline vehicles, point sources, and area sources decrease
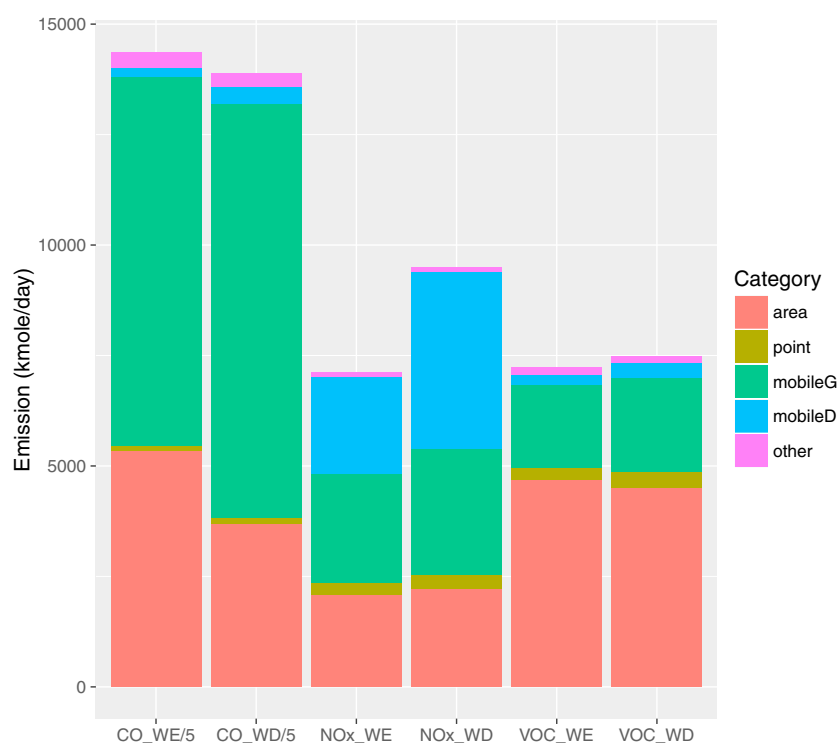
Figure 2. Average CO, NO_x, and VOCs emissions from various anthropogenic emission source categories in SoCAB on weekday and weekend during May to July 2010. Note that the CO emissions were divided by a factor of 5 in the plot in order to use the same y scale.

by 13%, 18%, and 6%, respectively, on weekends compared to weekdays. Total NO_x emissions on weekends are about 75% of the weekday emissions in SoCAB. Area source emissions are the dominant source of VOCs contributing approximately two thirds of the total VOCs on both weekdays and weekends. Key emitters of VOCs in area source category include off-road equipment and recreation vehicles, consumer product, and farm operation. On-road mobile emissions of VOCs are mostly from gasoline vehicles with a very small fraction from diesel vehicles. On weekends, area emissions of VOCs increase while mobile emissions of VOCs decrease compared to weekdays. These opposite trends result in a total decrease of VOCs on weekends of 4%.

It is well known that VOC species with different chemical structures vary significantly with respect to their reactivities and ozone forming potential in the presence of sufficient NO_x. One commonly used reactivity scale is Maximum Incremental Reactivity (MIR, Carter, 1994). Chemical mechanisms that are used in air quality models often have some explicit VOC species and some lumped species that represent species with similar structure and hydroxyl reactivities. Table 2 lists the averaged total emissions for key modeled VOCs species, both explicit and lumped, in SoCAB on weekdays and weekends from May to July 2010. MIR for each species and the MIR weighted emissions are also included in Table 2. When considering total molar emissions only, ALK4, ethanol, ALK1, ALK5, ethene, and ALK3 are the top six species with highest emissions. However, ethene, OLE2, propene, toluene, m-xylene, and ALK4 are the six species that have the highest MIR weighted emissions and thus have the highest O_3 forming potential. Table 2 shows that toluene and ALK4 emissions are about 5% lower on weekends than weekdays, while emissions for ethene, OLE2, propene, and m-xylene are higher on weekends than weekdays with the increase ranges from 1% to 6%.

In order to show the temporal and spatial variations of emissions in SoCAB, weekday and weekend diurnal patterns of NO_x and VOC emissions in the three SoCAB subregions are illustrated in Figure 3. The data are based on the average of the nine 4×4 km^2 grid cells surrounding each of the 21 monitoring sites where NO_x observations are available (seven sites for each subregion), as listed in Table S2. The associated weekly emission patterns for NO_x and VOCs are provided in Figure S2 in the supporting information. Spatially, NO_x and VOC emissions are highest in the region defined as coastal, followed by valley and inland regions as shown

Table 2

Weekday and Weekend Anthropogenic Emissions of NO_x, CO, VOCs (kmol/day) and the O_3 Formation Potentials for VOCs in SoCAB

		WD		WE		WE/WD
	Molar MIR	kmole	kmole O_3 potential	kmole	kmole O_3 potential	mole ratio
124-Trimethyl Benzene	22.2	30	667	29	642	0.96
m-Xylene	21.6	80	1729	82	1770	1.02
o-Xylene	16.9	44	740	43	719	0.97
1–3 Butadiene	14.2	21	298	28	398	1.33
p-Xylene	12.9	20	259	18	237	0.92
Propene	10.2	180	1832	191	1946	1.06
OLE2	9.8	205	2007	206	2018	1.01
RCHO	8.6	32	278	27	233	0.84
ARO2	8.4	91	761	89	746	0.98
Toluene	7.7	256	1972	244	1881	0.95
OLE1	6	91	544	92	551	1.01
Acetaldehyde	6	74	445	65	393	0.88
Formaldehyde	5.9	269	1586	248	1464	0.92
Ethene	5.3	534	2832	547	2898	1.02
MEK	5	45	226	36	178	0.79
ARO1	2.5	52	130	51	128	0.98
ALK4	1.5	1148	1722	1108	1661	0.96
Ethanol	1.5	1132	1699	1072	1608	0.95
ALK5	1.2	691	830	618	742	0.89
ALK3	1.2	516	619	506	607	0.98
Benzene	1.2	86	103	86	104	1.01
ALK2	0.5	297	149	292	146	0.98
Acetylene	0.5	186	93	187	94	1.01
Methanol	0.4	201	80	187	75	0.93
Acetone	0.4	232	93	210	84	0.90
ALK1	0.3	904	271	895	268	0.99
NO		8526		6410		0.75
NO_2		969		728		0.75
NO_x		9494		7139		0.75
CO		69424		71939		1.04
AVOC		7495	21965	7232	21591	0.96

Note. O_3 formation potentials are calculated by multiplying emissions of VOCs and their Maximum Incremental Reactivity (MIRs; mole O_3/mole VOC). RCHO: lumped C3+ aldehydes, ARO1–2: aromatics, ALK1–5: alkanes and other nonaromatics, OLE1–2: alkenes, MEK: ketones and other nonaldehyde oxygenated products.

in both Figures 3 and S2. Total daily NO_x emissions are substantially lower on Saturdays and Sundays than on weekdays in all the three subregions. The variability in emissions during weekdays is small, with Mondays generally having lowest emissions compared to other weekdays. VOC emissions on Saturdays and Sundays are slightly lower than weekdays. The diurnal plots in Figure 3 indicate that the reduced NO_x emissions on the weekend occur at all the hours of the day, whereas weekend VOC reduction mainly occurs during morning hours from 4:00 to 8:00.

4. Comparison Between Model Simulations and Observations

4.1. NO_2 and NO_x

NO_2 and NO_x data from model simulations for weekdays and weekends in SoCAB are compared with measurements from different observational platforms. These measurement platforms include (1) hourly mixing ratios of NO_2 and NO_x from 21 routine ground monitoring sites in SoCAB during May to July 2010; (2) NO_2 and NO_x mixing ratios measured at the Pasadena supersite from 16 May to 16 June 2010 (1-min measurements were averaged to one hour for comparison to the hourly model output); (3) NO_2 and NO_x concentrations measured from the P3 flights over the SoCAB domain for six weekdays (4, 14, 19, 21 May and 2, 3 June) and four weekend days (8, 16, 20, 30 May) during CalNex; Observed and modeled NO_2 and NO_x were further segregated to below and above 1 km to demonstrate the difference between air masses at lower and upper levels; (4) NO_2 vertical column below the Twin Otter aircraft measured by AMAX-DOAS for 26 days (18
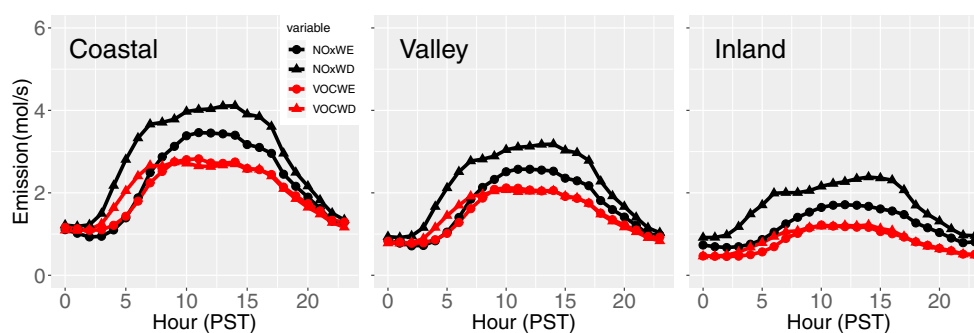
Figure 3. Average diurnal patterns of NO_x and VOC emissions in coastal, valley, and inland areas of SoCAB on weekdays and weekends during May–July 2010. Data are based on the average of 9 grid cells surrounding the 21 ground sites where NO_x observation are available (Table S2). Each area has seven monitoring sites. SoCAB = South Coast Air Basin.

weekdays and 8 weekends) during 23 May to 19 July 2010. Modeled data were extracted corresponding to each observation platform. For ground sites including the Pasadena supersite, modeled hourly data are used. For comparison with P3 measurements, we first extracted and interpolated the model data to reflect the time and location of the 1-s merged observation data. The 1-s data points that were within the same model grids were then averaged to calculate a single value for a grid cell. For the NO_2 column below the Twin Otter aircraft, measurements under solar zenith angles less than 30° have minimal retrieval errors and are selected for model comparison. The modeled NO_2 column was extracted based on the time and the footprint of the measurements. A detailed time series comparison of observed and modeled NO_2 and NO_x at Pasadena supersite is illustrated in Figure S3. Spatial distributions of NO_2 and NO_x below 1 km and above 1 km along P3 flights are shown in Figures S4 to S7. Vertical distribution of NO_2 and NO_x along P3 flights are shown in Figures S8 and S9. Spatial distributions of observed and modeled NO_2 columns below the Twin Otter are shown in Figure S10. Among all the measurement platforms, we consider the surface monitoring network to be the most representative of the actual WE/WD effect since it is the most robust in terms of the number of data points and spatial distribution and does not contain the potential inconsistencies in time and location of the WE/WD measurements inherent in the aircraft and column data.

4.1.1. Average NO_2 and NO_x and Their WE/WD Ratios From Model and Observation at Different Platforms

Average NO_2 and NO_x for weekdays and weekends from the model and observations and for different platforms are displayed in the top panel of Figure 4. The WE/WD ratios are compared in the bottom panel of Figure 4. On average, the top panel of Figure 4 shows that with a slight underprediction, the model captured near 90% or more of the NO_2 and NO_x mixing ratios that were observed at ground sites including routine monitoring sites and the Pasadena supersite. The agreement between the model and observations is better for weekends compared to weekdays. It is well known that ground measurement of NO_2 may be biased high due to the interference by an unquantifiable fraction of organic nitrate and nitric acid (Demerjian, 2000). Therefore, the agreement between the model and the true NO_2 mixing ratios may be better. The predicted and observed WE/WD ratios show excellent consistency at these ground sites. For NO_2, the observed WE/WD ratios are 0.75 and 0.72 at routine monitoring sites and Pasadena supersite, respectively, while the modeled ratios are 0.77 and 0.75, respectively. The WE/WD ratios for NO_x are slightly lower compared to NO_2, which is reasonable since NO_x emissions are primarily NO (i.e., much larger NO fraction). The observed ratios are 0.70 and 0.68 at routine monitoring sites and Pasadena supersite, respectively, while the modeled ratios are 0.73 and 0.71, respectively. NO_2, NO_x, and their WE/WD ratios at ground sites will be further investigated in the following section.

The observed and modeled NO_2 and NO_x data along the P3 flight tracks are segregated to below 1 km (shown as P3NO$_2$ConcL and P3NO$_x$ConcL in Figure 4) and above 1 km (shown as P3NO$_2$ConcU and P3NO$_x$ConcU in Figure 4). Note that the midday PBL height was roughly 1 km at Pasadena. The data from a limited number of flights show that during weekdays, average modeled P3NO$_2$ConcL and P3NO$_x$ConcL are about 77% and 84% of the observed values, respectively, which is consistent with the general underprediction at the ground sites. During the weekend, however, the average model results for both P3NO$_2$ConcL and
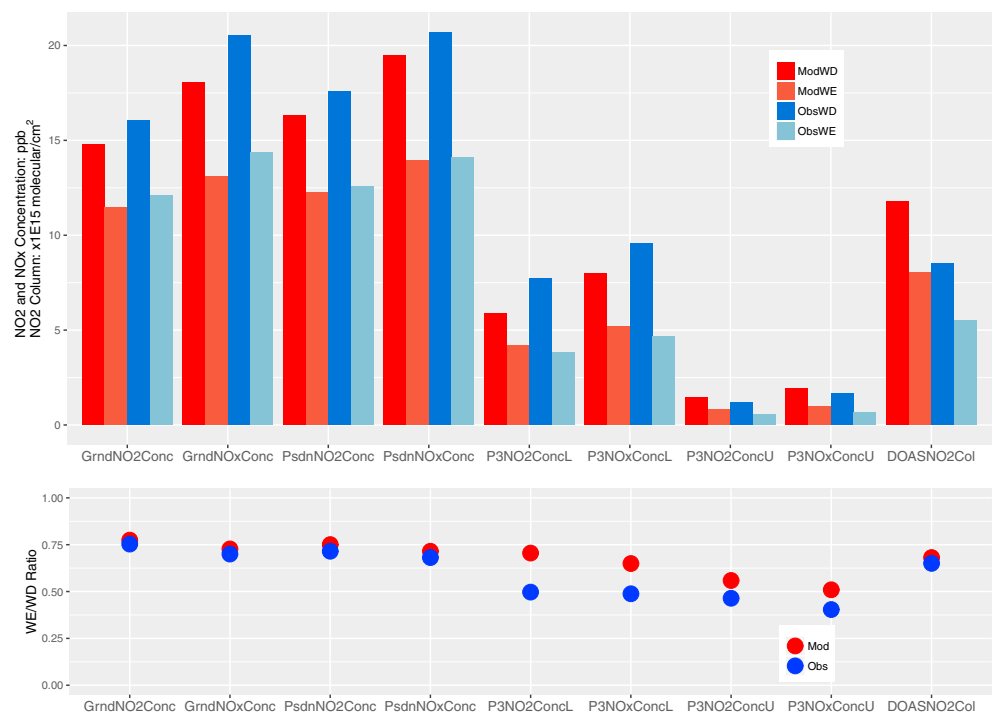
Figure 4. (top panel) Average observed and modeled NO_2 or NO_x on weekdays and weekends: (1) NO_2 and NO_x mixing ratios at routine ground sites (GrndNO$_2$Conc and GrndNO$_x$Conc), (2) NO_2 and NO_x mixing ratios at Pasadena supersite (PsdnNO$_2$Conc and PsdnNO$_x$Conc), (3) NO_2 and NO_x mixing ratios below 1 km along P3 flight track (P3NO$_2$ConcL and P3NO$_x$ConcL), (4) NO_2 and NO_x mixing ratios above 1 km along P3 flight track (P3NO$_2$ConcU and P3NO$_x$ConcU), and (5) AMAX-DOAS NO_2 column below Twin Otter airplane (DOASNO$_2$Col). (bottom panel) Observed and modeled weekend to weekday ratios at different platforms.

P3NO$_x$ConcL are biased high by 8%. The opposite biases for weekdays and weekends result in large differences between modeled and observed WE/WD ratios for P3NO$_2$ConcL and P3NO$_x$ConcL. The modeled WE/WD ratios for P3NO$_2$ConcL and P3NO$_x$ConcL are 0.71 and 0.65, respectively, which is within the same range as the ratios for the ground sites. However, the observed ratios are only around 0.5 for both P3NO$_2$ConcL and P3NO$_x$ConcL. Above 1 km, the averaged NO_2 and NO_x mixing ratios decrease significantly as compared to below 1 km. P3NO$_2$ConcU and P3NO$_x$ConcU are overpredicted in the model by about 20% for weekdays and 40% for weekends. The modeled WE/WD ratios for P3NO$_2$ConcU and P3NO$_x$ConcU are 0.55 and 0.51, respectively, both of which are slightly higher than the observed ratios of 0.46 and 0.40. Figures S8 and S9 suggest large variation of NO_2 and NO_x aloft, particularly for weekday observations. The shapes of vertical distributions also differ on weekdays and weekends indicating that different conditions might have been sampled as the aircraft sampled the aloft air mass over different locations and at different times. In addition, potential uncertainties with boundary conditions, vertical mixing, and local emissions may have also contributed to the larger discrepancies of WE/WD ratios between the model and observations aloft as compared to the surface sites.

In contrast to the overall underprediction at ground sites and below 1 km, the model overpredicted the NO_2 column below the Twin Otter aircraft by 39% on weekdays and by 29% on weekends. Figure S10 shows that the overprediction of the NO_2 column during weekdays is mostly in the Valley and Inland regions, while on weekends the overprediction is mostly in the coastal region. This overprediction of NO_2 column may partially be explained by the overprediction of NO_2 above 1 km as discussed above. However, the model data show that on average, 80% of the NO_2 column below Twin Otter is from NO_2 below 1 km. This difference in model biases for NO_2 mixing ratio and NO_2 column could also result from differences in flight dates/time for the P3 and Twin Otter as well as the uncertainties with different measuring techniques and will need further investigation. Despite the overprediction of NO_2 column data, the modeled WE/WD ratio is inline with the observed ratio and also in the same range as the WE/WD ratios for mixing ratios at ground sites.
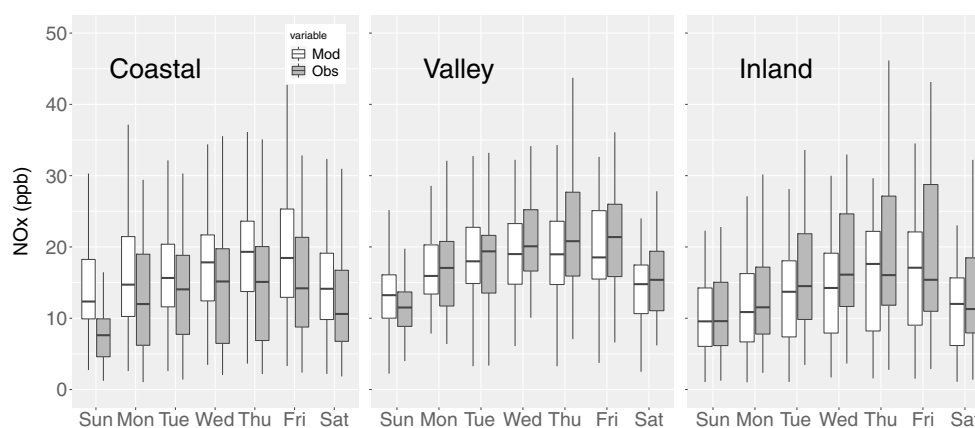
Figure 5. Observed and modeled weekly patterns of NO_x concentrations at the three subregions.

4.1.2. Weekly and Diurnal Patterns of NO_2 and NO_x at Routine Ground Sites

Day of week variations of NO_x from observations and the model simulation at the 21 routine ground sites are grouped into three subregions and illustrated in Figure 5. The data used in the figure include all the hourly data from May to July 2010. The day-of-week variations of NO_2 are similar to that of NO_x and are illustrated in Figure S11. Although NO_x emissions data (Figures 3 and S2) show the highest emissions in the coastal area, followed by the valley and inland regions, the NO_x mixing ratios generally fall within similar ranges among the subregions, with the valley having somewhat higher observed values and the coastal area having the lowest values. This illustrates the importance of the transport and redistribution of NO_x from its source regions to different areas in the air basin. In all three subregions, the observed NO_x mixing ratios start at their lowest values on Sunday and steadily accumulate through Thursday. The NO_x mixing ratios then decrease slightly on Friday with substantial drop on Saturday and into Sunday. The model successfully captured the day-of-week variation within all the three subregions. The modeled median mixing ratio for each day showed agreement to within 15% with the observations in the valley and inland areas with a slight underprediction on most days. NO_x mixing ratios were overpredicted in the coastal area with the median, 25%, and 75% quantiles from the model all showing higher values than those from the observations and for all days of the week. The overprediction of NO_x in the coastal region and underprediction in the valley and inland regions may be due to an underestimate in the transport of air masses from the coastal source region. Specifically, comparison between modeled and observed wind speeds at the Los Angeles airport and Santa Monica monitoring sites (not shown) suggests that WRF generally underestimated the wind speed for these coastal sites.

Diurnal variations of NO_x mixing ratio for the 21 routine monitoring sites for weekdays and weekends as well as the WE/WD ratios from the model and observations for the three subregions are illustrated in Figure 6. Similar diurnal plots for NO_2 are illustrated in Figure S12 in the supporting information. Observed data for 4:00 PST are not available for the majority of the sites, so data for that hour were excluded in the plot of the observed data. Weekday NO_x levels peak in all three subregions during morning rush hours. The peak times are 6:00 PST in valley and inland regions and 7:00 PST in coastal region reflecting the direction of morning traffic that is mainly from the east and north of the air basin to the metropolitan area along the western coast. The model successfully captured the timing of the NO_x peak, within 1 hr, with a slight overprediction in the coastal region and more substantial underpredictions in the valley and inland regions. For the daytime hours from 10:00 to 17:00 PST, modeled NO_x agreed well with the observations in the coastal region but was biased low for both valley and inland regions. During nighttime from 20:00 to 1:00 PST, when NO_2 is the dominant component of NO_x, the model overpredicted both NO_2 and NO_x but most significantly in the coastal region. This model discrepancy can be partially attributed to errors in the simulated PBL heights. During CalNex, PBL heights were measured using the ceilometer technique at the Pasadena supersite. The average diurnal patterns of PBL from the ceilometer measurement and WRF simulations are presented in Figure S13. Ceilometer measurement is more reliable for noon hours when the convective boundary layer is fully developed and less reliable
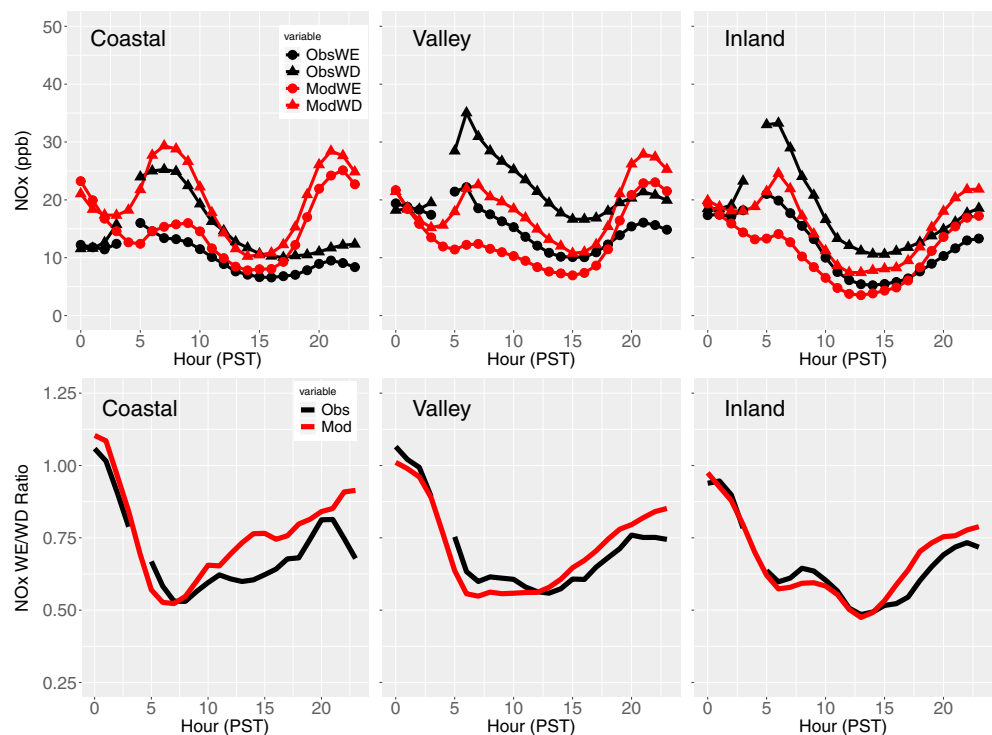
Figure 6. (top) Average diurnal patterns of NO$_x$ mixing ratios on weekdays and weekends from model and observation at the routine ground sites in the three subregions of SoCAB. (bottom) Average WE/WD ratios of NO$_x$ mixing ratio from model and observation. SoCAB = South Coast Air Basin.

during transition periods, such as morning hours when the boundary layer is developing and evening hours when it collapses (Eresmaa et al., 2012; Haman et al., 2012; Träumner et al., 2011). Schween et al. (2014) reported that the aerosol-based retrieval of the ceilometer measurement generally gives higher PBL heights than the measurements from a wind lidar. Given this limitation in the PBL height measurements, Figure S13 shows an overprediction of PBL during daytime hours near noon and an underprediction during nighttime. This behavior is consistent with the WRF simulation reported by Kelly et al. (2014) for their CalNex modeling and partially explains the underprediction during daytime and overprediction during nighttime for both NO$_x$ and NO$_2$. The daytime overprediction of PBL also partially explains the underprediction of P3 data below 1 km and overprediction above 1 km mentioned earlier.

Despite the model bias in simulating NO$_x$ and NO$_2$ mixing ratios, the diurnal patterns for WE/WD ratios from the model simulation are in excellent agreement with observations in the valley and inland regions but did exhibit a small overprediction after 15:00 PST. The better model performance for the WE/WD ratios compared to the absolute mixing ratios is likely due in part to errors in meteorology, such as PBL height, and transport, which are reduced in the WE/WD ratio calculation. The prediction of the WE/WD ratio in the coastal area agrees well with the observations from midnight to noon but is biased high after the noon hour. The larger model bias for WE/WD ratio in the coastal region compared to the other two regions may imply that while the emission inventory broadly captures the weekend versus weekday changes in NO$_x$, there are still potential uncertainties related to specific activities, such as emissions from vehicles traveling to and from the coastal beaches on the weekends, that are not well represented in the emissions inventory, as well as errors in simulating local meteorology, transport, deposition, etc. that may also play a role in causing the discrepancies. For all three subregions, the lowest WE/WD ratios can go as low as 0.48 (13:00 PST in the inland region) and the model predicted this reasonably well. The reduction of NO$_x$ during morning rush hours is most significant in the coastal region where both the model and observations see a minimum WE/WD ratio of 0.52 at 7:00 PST. Weekend changes of NO$_x$ during the nighttime hours are relatively small compared to the daytime. For some
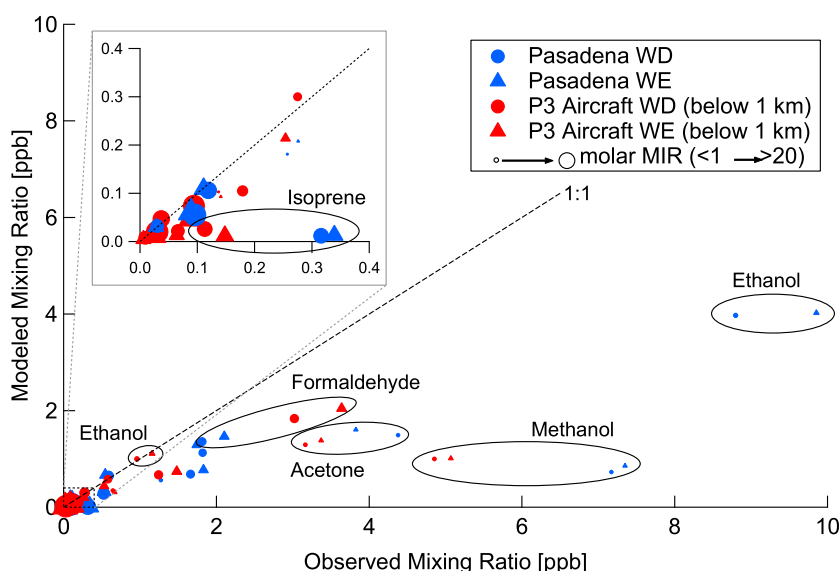
Figure 7. Scatterplot for the average mixing ratios of explicit VOC species from model versus average mixing ratios from observations at Pasadena supersite and along the P3 flight tracks during weekdays and weekends. Different sizes of symbols represent VOC species with different MIR values. VOC = volatile organic compound; MIR = Maximum Incremental Reactivity.

hours near midnight in the coastal and valley regions, both observations and the model show that the weekend NO_x can be even higher than on weekdays (WE/WD ratio greater than 1), which is indicative of the nighttime activities that produce more NO_x emissions on weekends.

4.2. VOC and CO

4.2.1. Comparison of Campaign Mean Concentrations

Scatterplot for the average mixing ratios of explicit VOC species from model versus average mixing ratios from observations at Pasadena supersite and along the P3 flight tracks during weekdays and weekends is shown in Figure 7. Corresponding mixing ratios of these VOC species and CO are displayed in Table S3 in the supporting information. At the Pasadena supersite, mp-xylene was measured instead of the explicit m-xylene and p-xylene measured by the P3. Therefore, the sum of modeled m-xylene and p-xylene is compared with the measured mp-xylene at the Pasadena site. Since biogenic VOCs (BVOCs), such as isoprene and α-pinene, were measured at both the Pasadena supersite and by the P3, they are included in Figure 7 and Table S3. However, any difference in weekday and weekend levels of BVOCs is due to meteorological effects and differences in the P3 flight track, rather than any inherent difference in emission activity.

At the Pasadena supersite, modeled CO mixing ratios are in agreement to within ±2% of the observations at the Pasadena site, and both show only a very minor increase of CO on weekends compared to weekdays. Model simulations for o-xylene, 1–3 butadiene, mp-xylene, formaldehyde, toluene, and benzene compare to the observations with mean biases within ±30% for both weekdays and weekends. Most of these species are of fossil fuel origin indicating that emissions from this sector are well characterized in the emission inventory. For the remaining three species that are of fossil fuel origin, 124-trimethyl benzene, propene, and ethene, the model captured about 55–65% of the observed mixing ratios.

Simulated acetaldehyde, acetylene, and ethanol exhibited similar underprediction with modeled mixing ratios about 40–45% of the observed mixing ratios. For acetone and methanol, the two species with low reactivities (low molar MIR in Table S3), the modeled mixing ratio is about one third of the observed mixing ratio for acetone, while the simulated methanol is an order of magnitude lower than observed mixing ratios. Major sources for ethanol, acetone, and methanol include emissions from living plants, industrial and bio-fuel emissions, and biomass burning emissions. Ethanol and acetone are also the key markers in volatile chemical products (McDonald et al., 2018). Previous studies have shown that the current knowledge of the budget and distribution of these three species is still very limited, and the quantification of the

emission source is largely uncertain (Galbally & Kirstine, 2002; Jacob et al., 2005; Kirstine & Galbally, 2012; Millet et al., 2010; Naik et al., 2010; Singh et al., 2000, 2004). Using 2011 national emission inventory (NEI) for anthropogenic emission, another CMAQ (version 5.0.2) modeling study for CalNex by Baker et al. (2015) also reported large underestimation of ethanol and methanol. A recent study by McDonald et al. (2018) suggests VOC emissions from volatile chemical products are twice as large as from mobile sources in United States and might be underestimated by factors of 2 to 3. In our current emission inventory, 47% of ethanol emissions in SoCAB are from gasoline mobile sources and 34% are from consumer products and coating solvents. Consumer products and coating make up 37% of the acetone emissions, while biogenic emissions comprise 31%. Roughly 78% of methanol emissions are from biogenic sources and 13% are from gasoline mobile sources. The major sinks for ethanol, acetone, and methanol are reactions with the hydroxyl radical (OH). As shown in the following section, the model-simulated OH radical mixing ratios are in agreement to within 60% of the observations; therefore, the larger discrepancy between modeled and observed mixing ratios for ethanol, acetone, and methanol is likely due more to uncertainties in the emissions from various sources than from errors in the chemistry resulting from discrepancy in the OH budget. Since oxidation of ethanol with the hydroxyl radical is an important source for the formation of acetaldehyde, the underestimation of ethanol may also contribute in part to the underestimation of acetaldehyde in the model.

Along the P3 flight tracks, the model-simulated CO mixing ratios are biased low by 10–15%. The model performance for VOCs along the P3 flight tracks below 1 km is inline with the model predictions for the Pasadena supersite, except for ethanol. The model simulations for ethanol are in reasonable agreement with the measurement from the whole air samplers on the P3, although the modeled data are biased significantly low at the Pasadena supersite compared to the measurement from gas chromatograph mass spectrometer instrument. However, measured ethanol from the whole air sampler is likely biased low since two other oxygenated VOCs—acetone and methanol—are 2 to 3 times lower from the whole air sampler than from the PTR-MS measurement. Unfortunately, the ethanol measurement is not available from the PTR-MS. Whole air sampler and PTR-MS are in good agreement with each other for other comeasured species: acetaldehyde, isoprene, benzene, and toluene. The large difference between the oxygenated VOC measurements from gas chromatograph mass spectrometer and whole air sampler underlines potential uncertainties associated with observations and the importance of an intercomparison between different measurement techniques, which is beyond the scope of this study.

Averaged isoprene mixing ratio was measured to be approximately 0.3 ppb at Pasadena, and the averaged aircraft measurement throughout the basin was about 4 times lower. Even with urban biogenic isoprene emissions increased by a factor of 2.5, modeled isoprene was still significantly lower compared to observed levels. The ratio between isoprene and the sum of its oxidation products methyl vinyl ketone (MVK) and methacrolein (MACR) are often used as an indicator of the aging of isoprene with higher ratios (≥ 1) indicating more fresh isoprene emissions and low ratios indicating regionally aged emissions (Hu et al., 2015). Mean isoprene/(MVK + MACR) ratio from observations at Pasadena was 1.44 implying significant local emission sources for isoprene that was likely from the trees surrounding the site. The model results show a much lower isoprene/(MVK + MACR) ratio of 0.056, implying modeled isoprene at this site is more likely from aged emissions. The discrepancy between the model and observed isoprene mixing ratio and isoprene/(MVK + MACR) ratio suggests that local emissions for isoprene might be highly underestimated at Pasadena, and a better understanding and quantification of urban biogenic emissions is warranted. In contrast to isoprene, with a factor of 2.5 adjustment for α-pinene emissions, our modeled α-pine mixing ratios agree with the observations very well in Pasadena and along the P3 flight tracks. The underestimation of urban biogenic emissions also likely contributes to the underpredictions of methanol and ethanol for which a significant portion of emissions are from biogenic sources.

4.2.2. Correlation Between VOC Species and CO

Mixing ratios of many anthropogenic VOCs correlate well with CO due to a commonality of emission sources. Enhancement ratios (ER) of various VOCs to CO are determined from the slope of the correlation between VOCs and CO. ERs under minimal chemical impact (e.g., during nighttime) are often used to determine the emission ratios of these species and verify emission inventories (Bon et al., 2011; Borbon et al., 2013; Warneke et al., 2007). Meanwhile, the correlations between various VOCs to CO also exhibit large variability and may be strongly affected by chemical transformation processes during the daytime. In Warneke et al., 2013, ERs of individual VOC to CO, especially those with high reactivity, are used as
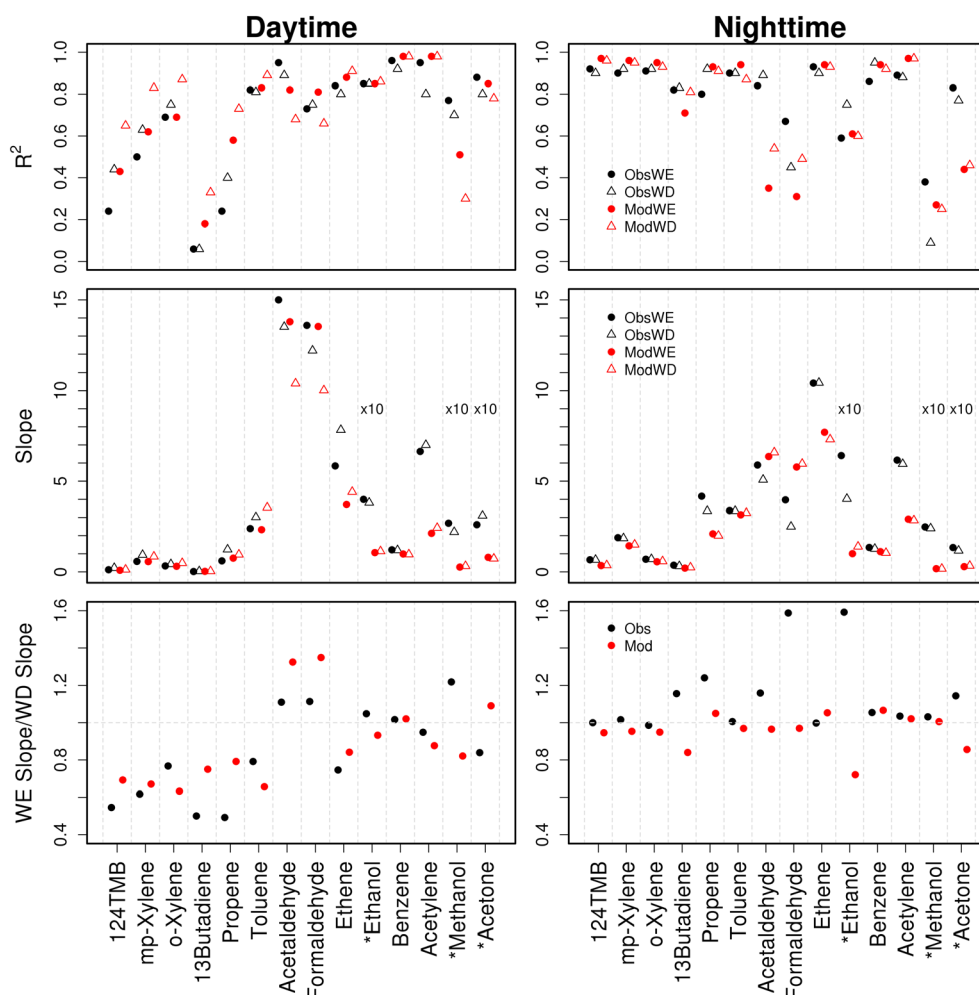
Figure 8. R^2, slopes, and WE/WD ratios of slopes of linear regression between various VOC species versus CO during daytime and nighttime on weekdays and weekends from model and observation at Pasadena supersite. Note that the slopes for ethanol, methanol, and acetone are scaled down by a factor of 10 to fit the plot scale. Values of the slopes and their 95th percentile confidential intervals are listed in Table S5. 124TMB: 124-trimethyl benzene. VOC = volatile organic compound.

indicators for the photochemical aging of VOCs in SoCAB on weekdays and weekends during CalNex 2010. In this section, we analyze the observed and modeled linear regressions between various VOC species and CO at the Pasadena supersite for both weekdays and weekends to investigate the modeling system's ability in capturing the emission and chemical characteristics of VOC compounds on weekdays and weekends. Data points for nighttime hours from midnight to 4:00 and daytime hours from noon to 16:00 were selected to represent photochemically inactive and photochemically active air masses, respectively. The daytime versus nighttime linear regression approach is based on the assumption that the relative VOC emissions to CO do not change between day and night (Borbon et al., 2013). Indeed, our analysis on the emission inventory shows a negligible change for emission ratios between daytime and nighttime. The correlation coefficients (R^2) and slopes of the linear regressions between VOC and CO emissions near Pasadena (nine grid cells surrounding Pasadena supersite) are provided in Table S4. We only segregate the emission data to weekday and weekend with no further separation between daytime and nighttime. The R^2 and slopes of the linear regression between 14 VOC species and CO from both the modeled and observed mixing ratios, and separated by weekdays and weekends, as well as the WE/WD ratios of the slopes, for both daytime and nighttime, are illustrated in Figure 8. Slopes and their 95th confidence intervals are also listed in Table S5 in the supporting information to further illustrate the statistical significance of difference between the slopes of various regression. Scatterplots for selected VOC species—

124-trimethyl benzene, mp-xylene, toluene, propene, formaldehyde, and benzene with CO—are illustrated in Figure S14 in the supporting information. A recent study by de Gouw et al. (2017) shows that the nighttime removal by ozone and nitrate (NO_3) radicals for highly reactive alkenes can be significant, which will impact the determination of emission ratios for those species. For the three alkene species—ethene, propene, and 1,3-Butadiene—that have low to moderate reactivities with O_3 and NO_3 during night, de Gouw et al. (2017) shows that considering the nighttime removal of these species will increase the emission ratio by about 10% compared to the slopes from linear regression approach in Borbon et al. (2013) and this work.

The R^2 of the linear regression between individual VOCs and CO in the emissions inventory is very close to 1.0 for all species shown in Table S4, which clearly indicates that the emissions of all 14 of the VOC compounds are strongly correlated with CO emissions near the Pasadena site (nine grid cells or 144 km^2 surrounding the supersite). For the emissions within the entire SoCAB domain, R^2 of the linear regression for most of the VOC species with CO are similar to those for Pasadena except for acetaldehyde, acetone, and methanol that have smaller R^2 values of 0.7, 0.5, and 0.7, respectively, reflecting sources other than fossil fuel burning (e.g., biogenic emissions or volatile chemical products, and others) for these species within the air basin.

During nighttime, VOC chemistry is minimal, and the ambient mixture of chemical compounds mostly reflects the emission sources. Figure 8 shows that the R^2 values for the linear regressions between mixing ratios of various VOCs and CO from model and observation are larger than 0.8 for 8 of the 14 VOC species for both weekday and weekend. For seven of the eight species (124-trimethyl benzene, mp-xylene, o-xylene, propene, ethene, benzene, and acetylene), the slopes of the correlation between the modeled mixing ratios with CO during nighttime are closely inline with the correlation between emissions of these species with CO and show only minor changes from weekday to weekend. Table S5 shows that the 95th percentile confidential intervals of modeled slopes are generally biased low compared to the intervals of observed slopes for these species suggesting that the emission ratios of these VOC species to CO could be underestimated in the model. For toluene, the modeled slopes during nighttime are 47% and 72% higher than the corresponding emission ratios for weekday and weekend, respectively, but modeled slopes and the WE/WD ratio are quite consistent with the observation. The slopes for the regressions of ethanol, methanol, and acetone as a function of CO are scaled down by a factor of 10 in Figure 8 to fit the scale used in the plot. The modeled slopes and their 95th percentile confidential intervals for these three species are biased significantly low compared to the observed slopes, indicating that there are uncertainties in the emissions of these species as well as the physical and chemical processes associated with these species. Modeled WE/WD ratio of slope is consistent with the observed WE/WD ratio for methanol but bias low for ethanol and acetone. These three species also exhibit higher modeled slopes than emission slopes during nighttime. Given the low reactivity of these species, this likely indicates that the site is being influenced by the transport of emissions from upwind sources that have a different mix of chemical species compared to the local sources. Formaldehyde and acetaldehyde are produced from the primary emission and the photochemical oxidation of other VOC compounds with OH radicals. During nighttime, the modeled mixing ratios of these two aldehydes and CO have R^2 values around 0.3 to 0.5 and the slopes are higher than the slopes of the regressions for the emission data, which suggests that residuals of these two species from daytime secondary formation may still be important at nighttime. The higher simulated slopes and their wider range of 95th percentile confidence intervals compared to observations at night for the two species suggest that there might be more sources impacting the site in the model, such as overestimated carryover from daytime to nighttime.

During daytime, the correlation coefficients for highly reactive VOCs (e.g., 124-trimethyl benzene, mp-xylene, oxylene, 1-3 butadiene, and propene) with CO are much smaller than the coefficients during nighttime due to the photochemical processes that are active during daytime hours. In Table S4, except for the four compounds with the lowest MIRs (benzene, acetylene, methanol, and acetone), the slopes and their 95th percentile confidence intervals for all the other primary VOCs with CO during the daytime are considerably lower than the slopes and confidence intervals for the nighttime. The daytime slopes for acetaldehyde and formaldehyde are more than twice the nighttime slopes, reflecting a strong production from chemical transformation. In contrast to the nighttime slopes, which show small weekend to weekday changes for most of the VOC species, the daytime slopes vary quite significantly during weekends compared to weekdays. The observed WE/WD ratios of the slopes range from 0.5 to 0.8 for the primary reactive species, while higher
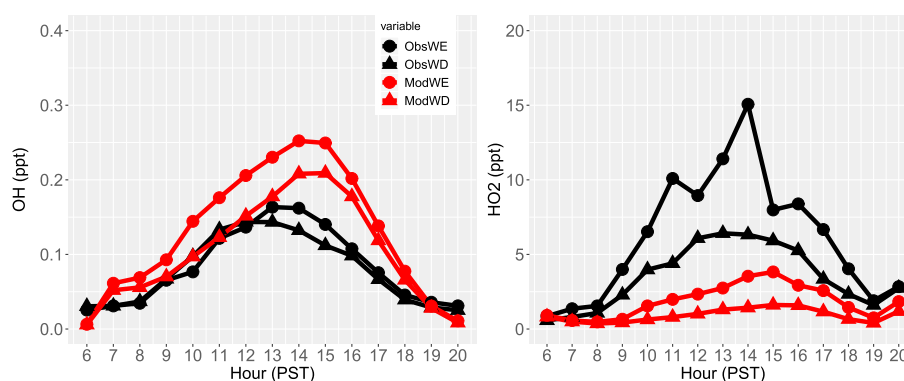
Figure 9. Average hourly OH and HO_2 mixing ratios at Pasadena site during weekdays and weekends.

ratios of 1.11 were observed for both acetaldehyde and formaldehyde, which is a strong indication for faster photochemical processes on weekends. Table S5 shows that the 95th percentile confidence intervals for modeled and observed slopes overlap with each other for most of the reactive species during the daytime indicating regressions for model and observation are statistically similar. The consistency between model and observation for R^2, slopes, and the WE/WD ratios of slopes for the reactive VOC suggests that the model is reasonably successful in reproducing the chemical characteristics of air masses under various conditions in a weekly cycle.

4.3. OH and HO_2 Radicals at the Pasadena Supersite

HO_x radicals play an essential role in the photochemistry of the atmosphere. Chemical transformation of VOCs and CO is initialized by the reactions with hydroxyl radicals. The oxidation of VOCs and CO by OH generates peroxy radicals (HO_2 and RO_2). Peroxy radicals can convert NO to NO_2 that then photolyzes to produce $O(^3P)$ and then O_3 by reacting with O_2. OH is recycled when HO_2 reacts with NO and is removed by reacting with NO_2 to form nitric acid. When the NO_x concentration is high on typical weekdays in SoCAB, OH formation is suppressed by removal from the reaction with NO_2. On weekends with low NO_x concentrations, the higher VOC/NO_x ratio favors the OH chemistry toward reacting with VOCs over reacting with NO_2, which promotes faster photochemical processes and results in lower concentrations for the reactive VOC compounds during daytime hours. Assuming negligible impact from mixing and dilution, and that emission ratios of VOCs to CO are identical to the ratios measured at Pasadena during the night, Warneke et al. (2013) used changes in the VOC to CO ratio to estimate an average of 65% higher OH on weekends compared to the same time period on weekdays due to weekend NO_x reductions.

OH and HO_2 radicals were measured at the Pasadena site during the CalNex campaign using laser-induced fluorescence-fluorescence assay by gas expansion technique (Griffith et al., 2016). Measured OH mixing ratios during nighttime are generally close or below detection limit, and the authors estimated that approximately 30% of the HO_2 measured are from interference with other peroxy radicals. Average measured hourly OH and HO_2 mixing ratios from 6:00 to 20:00 PST for weekdays and weekends are shown in Figure 9 along with the modeled data. For the HO_2 model comparison with observations, we applied a factor of 70% to the measured HO_2 to offset the interference from RO_2. It is unclear how the interference for the measurement may impact the model comparison with observation.

The measured OH mixing ratios show peaks near noon to 13:00 PST on average for both weekdays and weekends. Modeled OH generally peaks later than observed OH by 1 hr on weekdays and 2 hr on weekends. From early morning to noontime, measured OH mixing ratios do not show much change on weekends compared to weekdays. In the afternoon from 13:00 to 18:00 PST, measured weekend OH mixing ratios are higher than weekday mixing ratios. The average measured OH mixing ratios from noon to 16:00 PST (corresponding to our daytime VOC analysis above) are 0.126 and 0.142 ppt for weekdays and weekends, respectively, with an increase of 13% on weekends. Modeled weekday OH matches the observations for the morning hours on weekdays but is significantly higher than the observed OH in the afternoon. On weekends, modeled OH mixing ratios are clearly higher than the measurement for the daytime hours from 7:00 to 18:00 PST. Compared to the observation data, the modeled OH for the hours between 12:00 and
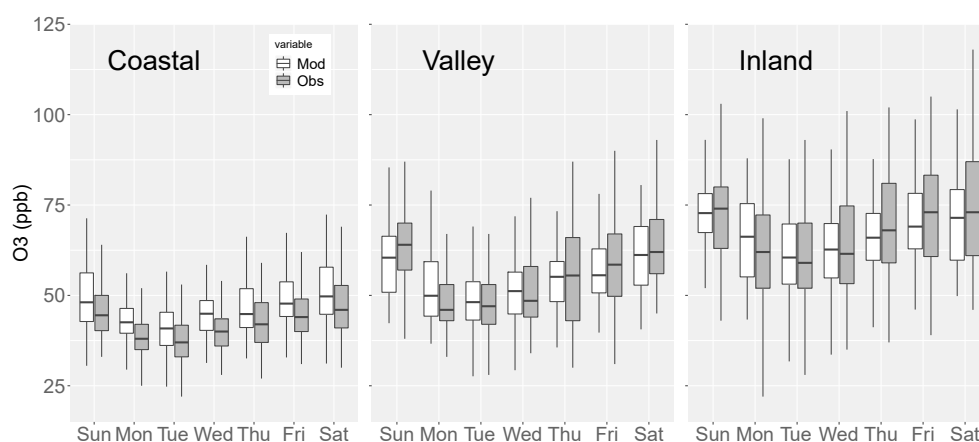
Figure 10. Observed and modeled weekly patterns of DM8hrO$_3$ at three subregions of SoCAB during May to July 2010. SoCAB = South Coast Air Basin.

16:00 PST is on average 51% and 88% higher for weekdays and weekends, respectively. The modeled data also exhibit much larger weekday versus weekend differences for OH than what were observed. The average modeled OH from noon to 16:00 PST is 0.19 on weekdays and 0.268 ppt on weekends, which is an increase of 44% on weekends compared to weekdays. This increase is much closer to the estimated 65% OH increase on weekends by Warneke et al. (2013) compared to the measured 13% OH increase. However, given the 1σ calibration accuracy of 18% in the OH measurements (Griffith et al., 2016), as well as the uncertainty associated with the method for estimating the change in OH described in Warneke et al. (2013) and the uncertainty associated with any photochemical modeling application (this work), it is difficult to say whether the relative change in OH calculated by the three methods is appreciably different.

For HO$_2$ mixing ratios, both the model and observations show distinct differences between weekdays and weekends, with higher HO$_2$ levels on weekends compared to weekdays. The average measured HO$_2$ mixing ratios from noon to 16:00 PST are approximately 6 and 10 ppt for weekdays and weekends, respectively, and represents a 67% increase on weekends. The model underpredicted HO$_2$ by nearly a factor of 3, with corresponding modeled HO$_2$ of 1.3 and 3 ppt for weekdays and weekends, respectively. The model simulated a weekend increase of 130% compared to weekdays. Collectively, our model overpredicts OH for most of the daytime hours but underpredicts HO$_2$ mixing ratios that are consistent with the results from Baker et al. (2015). The authors used the 2011 NEI for anthropogenic emission and SAPRC07TB chemical mechanism in the CMAQ simulation. SAPRC07TB is one of two variants of SAPRC07T mechanisms available in CMAQv5.0.2. The other is SAPRC07TC that is used in this work. The two variants have the same species and give similar predictions but differ in the numerical expression of reaction rate constants (Hutzell et al., 2012). The OH overprediction and HO$_2$ underprediction could be partially related to underprediction of VOC. But since during daytime, the biases for the reactive VOC species are mostly within $\pm$50%, the larger bias associated with HO$_x$ especially the underprediction of HO$_x$ by a factor of 3 is more likely due to the errors associated with the OH-HO$_2$ cycling in the chemical mechanism, which will require further investigation.

4.4. O$_3$

Day of the week variation in observed and modeled daily maximum 8-hr ozone (DM8hrO$_3$) from the routine ground measurement network is illustrated in Figure 10 for each of the three SoCAB subregions. The plots clearly show the spatial variation in the O$_3$ concentrations among the three subregions. O$_3$ concentrations are generally lowest in the coastal area followed by the valley and then inland, which exhibits the highest O$_3$ concentrations. In general, Tuesdays usually exhibit the lowest O$_3$ concentrations, with O$_3$ levels gradually increasing throughout the week and peaking on Sunday. Monday O$_3$ concentrations are significantly lower than Sunday but still higher than Tuesdays, presumably due to carryover from the preceding Sunday. The model was able to accurately capture the weekly cycles of O$_3$ in all three subregions. In the coastal area, the modeled median DM8hrO$_3$ values are a few parts per billion higher than observed for each day, while the model bias for the valley and inland varies depending on the day of week. In the valley, the
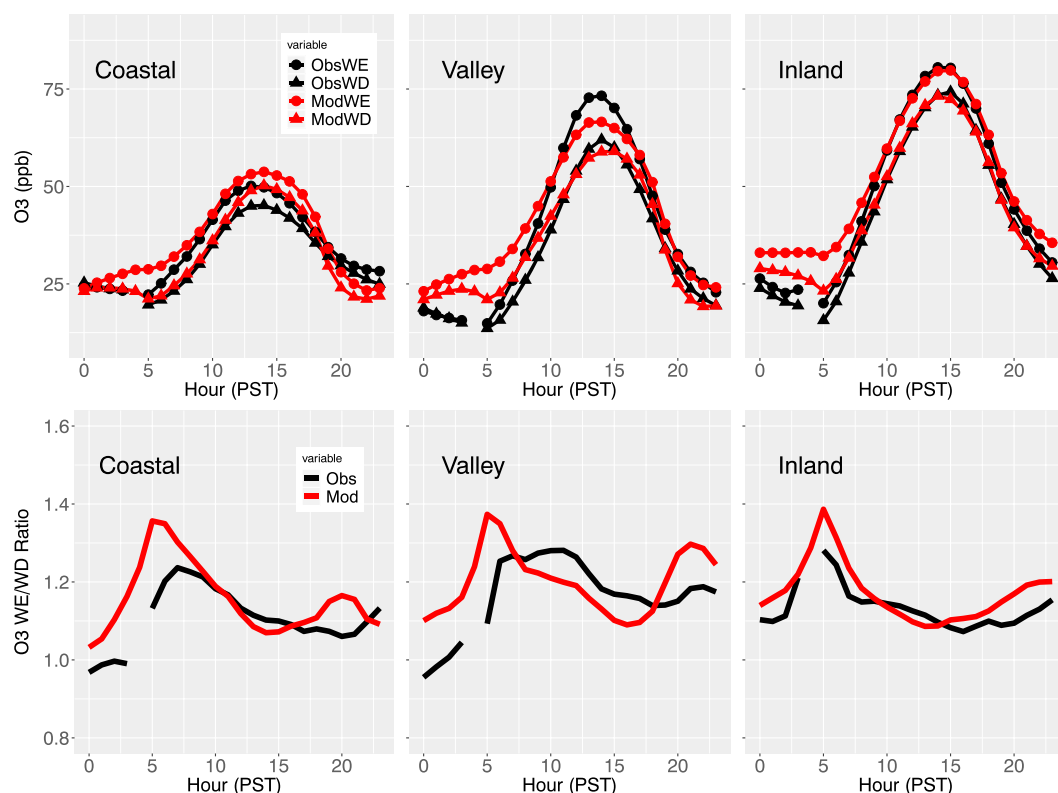
Figure 11. (top) Average diurnal pattern of O_3 mixing ratios on weekdays and weekends from model and observation at the routine ground sites in the three subregions of SoCAB. (bottom) Average WE/WD ratios of O_3 mixing ratio from model and observation. SoCAB = South Coast Air Basin.

median modeled $DM8hrO_3$ matches the observations well from Tuesday to Saturday but is biased low on Sunday and high on Monday. In the inland region, the median modeled $DM8hrO_3$ is generally inline with the observations but the modeled data show less variability as compared to the observations and did not capture the high end of the $DM8hrO_3$ distribution (top of the upper whisker in the boxplot). In each of the three subregions, the modeled median, 25%, and 75% quantile $DM8hrO_3$ on Monday are always higher than the observations, which may suggest the impact from the preceding Sunday on Monday is stronger in the model than was observed.

Observed and modeled diurnal patterns of hourly O_3 concentrations for both weekdays and weekends are shown in Figure 11 for each of the three subregions. The observation data indicate that in all three regions, the weekday and weekend O_3 concentrations are consistent with each other from midnight to 5:00 PST. Starting from 6:00 PST, O_3 accumulates much faster on weekends than weekdays as a result of less titration with NO and faster photochemical processes. The peak O_3 was mostly observed around 14:00 PST on both weekdays and weekends. The model successfully simulated the diurnal pattern of O_3 with some discrepancies. While the timing of the daily O_3 peak was well captured by the model, averaged daily peak O_3 mixing ratios were overpredicted near the coast, underpredicted in the valley, and reasonably well predicted inland. During 10:00 to 17:00 PST when the air mass is most photochemically active, the diurnal patterns of O_3 WE/WD ratio show that the valley region has the highest observed weekday to weekend differences with ratios ranging from 1.15 to 1.3. The model mostly underpredicted the daytime WE/WD ratio in the valley but exhibits good agreement with the daytime observed ratio for the coastal and inland regions. During the nighttime, when O_3 mixing ratios are low, the model generally simulated larger WE/WD ratios compared to the observations for all three regions.

Average $DM8hrO_3$ for all the ground monitoring sites on weekdays and weekends and the WE/WD ratio of $DM8hrO_3$ are listed in Table 3. On average, the observed WE/WD ratios of $DM8hrO_3$ for the valley, coastal, and inland regions were 1.16, 1.10, and 1.08, respectively, while the corresponding modeled ratios are 1.12,

Table 3
Average Daily Maximum 8-hr O_3 (DM8hrO_3) on Weekdays and Weekends From Model and Observation at Routine Ground Sites in SoCAB During May–July 2010

Region	Site	Observation			Model		
		WD	WE	WE/WD	WD	WE	WE/WD
Valley	Santa Clarita	60.6	67.3	1.11	59.4	62.3	1.05
	Reseda	58.7	61.7	1.05	57.4	59.2	1.03
	Burbank-W Palm Avenue	49.8	59.3	1.19	48.0	54.7	1.14
	Azusa	45.7	57.6	1.26	49.3	57.5	1.17
	Glendora-Laurel	54.6	66.4	1.22	52.1	60.6	1.16
	Pomona	51.2	58.6	1.14	52.7	62.4	1.18
	Pasadena-S Wilson Avenue	46.7	55.0	1.18	46.9	54.3	1.16
	Average	**52.5**	**60.8**	**1.16**	**52.2**	**58.7**	**1.12**
Coastal	West Los Angeles-VA Hospital	45.7	48.7	1.07	45.1	49.5	1.10
	Los Angeles-North Main Street	40.5	47.8	1.18	40.6	48.2	1.19
	Los Angeles-Westchester Parkway	41.8	43.3	1.04	45.6	48.7	1.07
	Pico Rivera-4144 San Gabriel	38.9	46.5	1.20	46.4	53.4	1.15
	North Long Beach	37.0	41.2	1.11	42.0	46.7	1.11
	La Habra	46.2	52.3	1.13	47.6	55.2	1.16
	Costa Mesa-Mesa Verde Drive	43.2	45.2	1.05	46.7	49.6	1.06
	Mission Viejo-26081 Via Pera	48.7	51.6	1.06	52.5	56.6	1.08
	Average	**42.8**	**47.1**	**1.10**	**45.8**	**51.0**	**1.11**
Inland	Lake Elsinore-W Flint Street	58.2	58.6	1.01	66.5	66.8	1.01
	Perris	67.5	66.7	0.99	68.3	70.2	1.03
	Riverside-Rubidoux	65.0	70.1	1.08	62.3	68.5	1.10
	Crestline	71.0	74.6	1.05	62.8	71.3	1.13
	Fontana-Arrow Highway	56.7	68.3	1.21	56.8	66.3	1.17
	Redlands-Dearborn	65.6	72.2	1.10	65.6	72.4	1.10
	San Bernardino-4th Street	60.0	69.1	1.15	62.9	70.7	1.12
	Upland	57.8	68.9	1.19	54.8	64.4	1.17
	Banning Airport	70.3	68.3	0.97	69.0	68.6	0.99
	Average	**63.6**	**68.5**	**1.08**	**63.2**	**68.8**	**1.09**

1.11, and 1.09, respectively. The relatively lower WE/WD ratios observed inland, and particularly the ratios of 0.99 and 0.97 at the Perris and Banning airport monitors, indicate a weakening of the weekend ozone effect in the eastern part of the SoCAB. The analysis in Baidar et al. (2015) suggests that the weakening of weekend ozone effect in eastern SoCAB may be related to a higher occurrence of hot temperatures. Our model was able to capture the reduction in O_3 mixing ratio on the weekend at the Banning airport, with a WE/WD ratio of 0.99, but was unable to capture the ozone reduction at the Perris monitor, with a simulated WE/WD ratio of 1.03.

Figure 12 shows the vertical distributions of O_3 along P3 flight track from model and observations for weekdays and weekends. The corresponding spatial distribution of the data is illustrated in Figure S15 in supporting information. For weekday flights, the modeled O_3 mixing ratios are in nice agreement with the observations in both vertical and horizontal extents, except that the model missed the highest weekday O_3 of 94 ppb that was observed 4.3 km aloft east of Palm Spring. Nevertheless, the model successfully captured the overall enhancement of O_3 near that region as shown in Figure S15. Along the weekend flights, O_3 mixing ratios are substantially higher than the O_3 along the weekday flights in both the model and observations. The right panel of Figure 12 shows that the modeled O_3 mixing ratios are in agreement to within 15% with the observations below 2.5 km, whereas a systematic underprediction occurs above 2.5 km. The relatively lower O_3 mixing ratios below 0.5 km were mostly measured over the coastal region and were overpredicted in the model. High O_3 mixing ratios up to 104 ppb near 1 km aloft were observed mostly near the foothills and riverside in the inland region during the 8 and 16 May flights. Although the model underpredicted these highest O_3 mixing ratios, the model successfully simulated the enhanced O_3 over these regions at the altitude near 1 km (Figure S16). Overall, the model exhibits better performance simulating air masses below 2.5 km
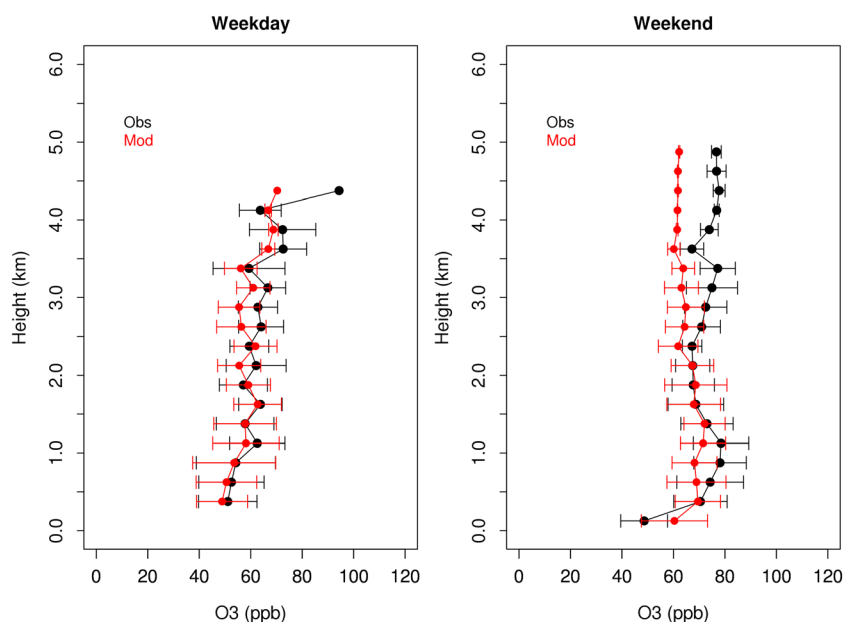
Figure 12. Vertical distributions of modeled and observed O_3 on weekdays and weekends along P3 flight tracks. Data are binned to every 250 m. Dots represent mean of each bin, and the error bars are $\pm\sigma$ for each bin.

than air masses above 2.5 km for both weekday and weekend. On average, observed O_3 mixing ratios are 59 and 74 along weekday and weekend flights, respectively, which equates to a 25% increase on weekends compared to weekdays. The corresponding average modeled O_3 mixing ratios are 56 and 67, respectively, or a 20% increase on weekends compared to weekdays. The limited data along P3 flights show both modeled and observed WE/WD ratios of O_3 aloft are higher than the average WE/WD ratio of 1.11 at ground sites (Table 3). The higher WE/WD ratios of O_3 aloft compared to the surface measurements appear consistent with lower WE/WD ratios of NO_2 and NO_x aloft compared to the ground monitors given that the region is predominantly VOC limited with respect to ozone formation. Figure 4 shows that weekend reduction ratios for NO_2 and NO_x along the P3 flight tracks are significantly higher than the reduction ratios at ground sites. Along the P3 flight track, the model simulated less NO_2 and NO_x reductions on weekends that also partly explain the lower O_3 increase in the model as compared to the observation.

5. Summary and Discussion

The CARB's 2010 emission inventory shows a 30% reduction of NO_x, 4% reduction of total anthropogenic VOC, and 4% increase of CO emissions on weekends as compared to weekdays in SoCAB during the May to July 2010 period. As a result, measurement data from the CalNex 2010 field campaign and routine ground sites for various chemical compounds show distinct features for the NO_x-VOC-HO_x-O_3 photochemical system on weekends compared to weekdays. The extensive measurement data collected during CalNex also provide an excellent opportunity to evaluate a modeling system's ability to simulate O_3 precursor species, intermediate chemical compounds, and secondary pollutants, and more importantly, the response of these chemical compounds to the weekday versus weekend emission changes.

The modeled daily averages of NO_2 and NO_x are in agreement to within 10% with the observations at ground sites, including routine monitoring sites and the Pasadena supersite. For NO_2 and NO_x aloft, the modeled mixing ratios were biased low below 1 km and biased high above 1 km as compared to the measurements obtained on the P3 aircraft. The model significantly overpredicted NO_2 columns below the Twin Otter aircraft. Despite the differences in predicting the absolute NO_2 mixing ratios and NO_2 column densities, the modeled WE/WD ratio for NO_2 at the surface and NO_2 column remained highly consistent with the observed ratios and well inline with the WE/WD NO_x (NO_2) emission ratio of 75% for the SoCAB domain.

The diurnal plots of NO_2 and NO_x show that there is a general underprediction of NO_2 (NO_x) during daytime and an overprediction during many of the nighttime hours. These discrepancies are likely due in part to uncertainty in the prediction of the PBL that may be overestimated during the daytime and underestimated during the nighttime hours. The predictions of the diurnal patterns of WE/WD ratios for NO_2 and NO_x are less sensitivity to errors in predicted PBL heights and so are in very good agreement with the observed ratios.

The modeling system exhibited a reasonable performance in simulating the VOC compounds with fossil fuel origins but had a large bias in simulating certain species with mixed emission sources such as ethanol, methanol, and acetone with relatively low reactivities, suggesting that a better understanding of emission sources for these species is needed. Weekend versus weekday changes of enhancement ratios for various VOC species to CO clearly show faster photochemical processing on weekends, which is associated with higher OH mixing ratios, and the modeling system shows satisfactory performance in this regard. The model overpredicted OH and underpredicted HO_2 at the Pasadena ground supersite and also had larger WE/WD ratios for both radicals compared to the observations. This may indicate potential errors in the chemical mechanisms associated with HO_x chemistry and also suggest further investigation is needed to get insight into how the bias of HO_x may related to biases with VOCs and NO_x simulations. Although the focus of this work is anthropogenic VOC species, we found very significant underestimation of isoprene at the Pasadena supersite even after we applied a factor of 2.5 increase to urban isoprene emissions. A better understanding of the urban biogenic emissions and their role in local ozone chemistry is needed to improve air quality modeling in the SoCAB.

Weekly cycles and diurnal patterns of O_3 were well simulated by the model, as well as the spatial variation of O_3 throughout the SoCAB. Although average $DM8hrO_3$ was generally overpredicted near the coast, underpredicted in the valley, and predicted well across the inland region, the modeled WE/WD ratios for ozone were mostly consistent with the observations in all three regions. A decrease in $DM8hrO_3$ on weekends compared to weekdays was observed at two inland sites, suggesting this area may be transitioning to NO_x-limited chemical regime. The model captured the weekend decrease of $DM8hrO_3$ at one site but failed at another site. With limited data along the P3 flights, both the model and observations show higher weekend O_3 increases (ratios) as compared to the ground sites, consistent with higher NO_2 and NO_x weekend reductions along the P3 flight as compared to the ground sites.

Overall, mixing ratios for different chemical compounds from our model simulation exhibit various biases compared to the observation data across different measurement platforms. However, the model results show a robust ability to simulate the weekend effect, for a majority of the relevant chemical species in the atmosphere, resulting from changes in emissions for precursor species on the weekend. The ability of the modeling system to capture relative changes in atmospheric pollutants lends support to emission control targets, which are developed using models in a relative sense per United States EPA guidance (United States Environmental Protection Agency, 2018). Our study also suggests that improvements in meteorology, such as more accurate modeling of the PBL height, chemical processes (e.g., OH-HO_2 cycling), and a better quantification of noncombustion related emissions, will greatly benefit future improvements in air quality modeling.

Our future work will investigate how the anticipated updates to the California emissions inventory will improve the performance of the modeling system with respect to absolute mixing ratios of various chemical compounds as well as their WE/WD ratios, both of which are crucial for gaining confidence in a model's ability to be used to inform policy making. In particular, the mobile source inventory will be updated once the EMFAC2017 model (https://www.arb.ca.gov/msei/categories.htm#emfac2017) is approved for use by the United States EPA, as will the consumer products VOC inventory once the 2013/2014 consumer product survey results (https://www.arb.ca.gov/consprod/consprod.htm) are mined to update emission estimates as well as the relevant speciation profiles. Lastly, work is ongoing to update the biogenics inventory in California, with a focus on urban biogenic emissions, and preliminary results suggest that these updates result in a significant improvement in simulated ambient concentrations of biogenic compounds such as isoprene at the Pasadena supersite.

Disclaimer

This paper has been reviewed by the staff of the California Air Resources Board and has been approved for publication. Approval does not signify that the contents necessarily reflect the views and policies of the

California Air Resources Board, nor does mention of trade names or commercial products constitute endorsement or recommendation for use.

References

Altshuler, S. L., Arcado, T. D., & Lawson, D. R. (1995). Weekend vs. weekday ambient ozone concentrations: Discussion and hypotheses with focus on Northern California. *Journal of the Air & Waste Management Association*, *45*, 967–972.

Angevine, W. M., Eddington, L., Durkee, K., Fairall, C., Bianco, L., & Brioude, J. (2012). Meteorological model evaluation for CalNex 2010. *Monthly Weather Review*, *140*(12), 3885–3906. https://doi.org/10.1175/MWR-D-12-00042.1

Appel, K. W., Pouliot, G. A., Simon, H., Sarwar, G., Pye, H. O. T., Napelenok, S. L., et al. (2013). Evaluation of dust and trace metal estimates from the Community Multiscale Air Quality (CMAQ) model version 5.0. *Geoscientific Model Development*, *6*, 883–899. https://doi.org/10.5194/gmd-6-883-2013

Austin, J., & Tran, H. (1999). *A characterization of the weekend-weekday behavior of ambient ozone concentrations in California Technical Support and Planning Division*. Sacramento, CA: Calilfornia Air Resources Board.

Baidar, S., Hardesty, R. M., Kim, S.-W., Langford, A. O., Oetjen, H., Senff, C. J., et al. (2015). Weakening of the weekend ozone effect over California's South Coast Air Basin. *Geophysical Research Letters*, *42*, 9457–9464. https://doi.org/10.1002/2015GL066419

Baker, K. R., Carlton, A. G., Kleindienst, T. E., Offenberg, J. H., Beaver, M. R., Gentner, D. R., et al. (2015). Gas and aerosol carbon in California: Comparison of measurements and model predictions in Pasadena and Bakersfield. *Atmospheric Chemistry and Physics*, *15*(9), 5243–5258. https://doi.org/10.5194/acp-15-5243-2015

Baker, K. R., Misenis, C., Obland, M. D., Ferrare, R. A., Scarino, A., & Kelly, J. T. (2013). Evaluation of surface and upper air fine scale WRF meteorological modeling of the May and June 2010 CalNex period in California. *Atmospheric Environment*, *8*, 299–309.

Blanchard, C. L., & Tanenbaum, S. J. (2003). Differences between weekday and weekend air pollutant levels in Southern California. *Journal of the Air & Waste Management Association*, *53*(7), 816–828. https://doi.org/10.1080/10473289.2003.10466222

Bon, D. M., Ulbrich, I. M., de Gouw, J. A., Warneke, C., Kuster, W. C., Alexander, M. L., et al. (2011). Measurements of volatile organic compounds at a suburban ground site (T1) in Mexico City during the MILAGRO 2006 campaign: Measurement comparison, emission ratios, and source attribution. *Atmospheric Chemistry and Physics*, *11*(6), 2399–2421. https://doi.org/10.5194/acp-11-2399-2011

Borbon, A., Gilan, J., Kuster, W., Grand, N., Chevaillier, S., Colomn, A., et al. (2013). Emission ratios of anthropogenic volatile organic compounds in northern mid-latitude megacities: Observations versus emission inventories in Los Angeles and Paris. *Journal of Geophysical Research: Atmospheres*, *118*, 2041–2057. https://doi.org/10.1002/jgrd.50059

Carter, W. P. L. (1994). Development of ozone reactivity scales for volatile organic compounds. *Journal of the Air & Waste Management Association*, *44*, 881–899.

Chen, D., Li, Q., Stutz, J., Mao, Y., Zhang, L., Pikelnaya, O., et al. (2013). WRF-Chem simulation of NO_x and O_3 in the L.A. Basin during CalNex-2010. *Atmospheric Environment*, *81*, 421–432. https://doi.org/10.1016/j.atmosenv.2013.08.064

Chinkin, L. R., Coe, D. L., Funk, T. H., Hafner, H. R., Robert, P. T., Ryan, P. A., & Lawson, D. R. (2003). Weekday versus weekend activity patterns for ozone precursor emissions in California's South Coast Air Basin. *Journal of the Air & Waste Management Association*, *53*(7), 829–843. https://doi.org/10.1080/10473289.2003.10466223

Cleveland, W. S., Graedel, T. E., Kleiner, B., & Warner, J. L. (1974). Sunday and workday variations in photochemical air pollutants in New Jersey and New York. *Science*, *186*(4168), 1037–1038. https://doi.org/10.1126/science.186.4168.1037

Colman, J. J., Swanson, A. L., Meinardi, S., Sive, B. C., Blake, D. R., & Rowland, F. S. (2001). Description of the analysis of a wide range of volatile organic compounds in whole air samples collected during PEM-Tropics A and B. *Analytical Chemistry*, *73*(15), 3723–3731. https://doi.org/10.1021/ac010027g

de Gouw, J., & Warneke, C. (2007). Measurements of volatile organic compounds in the Earth's atmosphere using proton-transfer-reaction mass spectrometry. *Mass Spectrometry Reviews*, *26*(2), 223–257. https://doi.org/10.1002/mas.20119

de Gouw, J. A., Gilman, J. B., Kim, S.-W., Lerner, B. M., Isaacman-VanWertz, G. A., McDonald, B. C., et al. (2017). Chemistry of volatile organic compounds in the Los Angeles basin: nighttime removal of alkenes and determination of emission ratios. *Journal of Geophysical Research: Atmospheres*, *122*, 11,843–11,861. https://doi.org/10.1002/2017JD027459

Demerjian, K. L. (2000). A review of national monitoring networks in North America. *Atmospheric Environment*, *34*, 1861–1884.

Dusanter, S., Vimal, D., Stevens, P. S., Volkamer, R., & Molina, L. T. (2009). Measurements of OH and HO_2 concentrations during the MCMA-2006 field campaign—Part 1: Deployment of the Indiana University laser induced fluorescence instrument. *Atmospheric Chemistry and Physics*, *9*(5), 1665–1685. https://doi.org/10.5194/acp-9-1665-2009

Elkus, B., & Wilson, K. R. (1977). Photochemical air pollution: Weekend-weekday differences. *Atmospheric Environment*, *11*(6), 509–515. https://doi.org/10.1016/0004-6981(77)90067-1

Emmons, L. K., Walters, S., Hess, P. G., Lamarque, J.-F., Pfister, G. G., Fillmore, D., et al. (2010). Description and evaluation of the Model for Ozone and Related chemical Tracers, version 4 (MOZART-4). *Geoscientific Model Development*, *3*(1), 43–67. https://doi.org/10.5194/gmd-3-43-2010

Ensberg, J. J., Craven, J. S., Metcalf, A. R., Allan, J. D., Angevine, W. M., Bahreini, R., et al. (2013). Inorganic and black carbon aerosols in the Los Angeles basin during CalNex. *Journal of Geophysical Research: Atmospheres*, *118*, 1777–1803. https://doi.org/10.1029/2012JD018136

Eresmaa, N., Härkönen, J., Joffre, S., Schultz, D., Karppinen, A., & Kukkonen, J. (2012). A three-step method for estimating the mixing height using ceilometer data from the Helsinki testbed. *Journal of Applied Meteorology and Climatology*, *51*, 2172–2187. https://doi.org/10.1175/JAMCD-12-058.1

Fast, J. D., Allan, J., Bahreini, R., Craven, J., Emmons, L., Ferrare, R., et al. (2014). Modeling regional aerosol and aerosol precursor variability over California and its sensitivity to emissions and long-range transport during the 2010 CalNex and CARES campaigns. *Atmospheric Chemistry and Physics*, *14*(18), 10,013–10,060. https://doi.org/10.5194/acp-14-10013-2014

Finlayson-Pitts, B. J., & Pitts, J. J. N. (1986). *Atmospheric chemistry: Fundamentals and experimental techniques*. New York: John Wiley.

Fujita, E. M., Stockwell, W. R., Campbell, D. E., Keislar, R. E., & Lawson, D. R. (2003). Evolution of the magnitude and spatial extent of the weekend ozone effect in California's South Coast Air Basin, 1981–2000. *Journal of the Air & Waste Management Association*, *53*(7), 802–815. https://doi.org/10.1080/10473289.2003.10466225

Galbally, I. E., & Kirstine, W. (2002). The production of methanol by flowering plants and the global cycle of methanol. *Journal of Atmospheric Chemistry*, *43*(3), 195–229. https://doi.org/10.1023/A:1020684815474

Gerbig, C., Schmitgen, S., Kley, D., Volz-Thomas, A., Dewey, K., & Haaks, D. (1999). An improved fast-response vacuum-UV resonance fluorescence CO instrument. *Journal of Geophysical Research*, *104*(D1), 1699–1704. https://doi.org/10.1029/1998JD100031

Gilman, J. B., Burkhart, J. F., Lerner, B. M., Williams, E. J., Kuster, W. C., Goldan, P. D., et al. (2010). Ozone variability and halogen oxidation within the Arctic and sub-Arctic springtime boundary layer. *Atmospheric Chemistry and Physics*, *10*(21), 10,223–10,236. https://doi.org/10.5194/acp-10-10223-2010

Griffith, S. M., Hansen, R. F., Dusanter, S., Michoud, V., Gilman, J. B., Kuster, W. C., et al. (2016). Measurements of hydroxyl and hydroperoxy radicals during CalNex-LA: Model comparisons and radical budgets. *Journal of Geophysical Research: Atmospheres*, *121*, 4211–4232. https://doi.org/10.1002/2015JD024358

Guenther, A., Karl, T., Harley, P., Wiedinmyer, C., Palmer, P. I., & Geron, C. (2006). Estimates of global terrestrial isoprene emissions using MEGAN (Model of Emissions of Gases and Aerosols from Nature). *Atmospheric Chemistry and Physics*, *6*(11), 3181–3210. https://doi.org/10.5194/acp-6-3181-2006

Haman, C. L., Lefer, B., & Morris, G. A. (2012). Seasonal variability in the diurnal evolution of the boundary layer in a near-coastal urban environment. *Journal of Atmospheric and Oceanic Technology*, *29*(5), 697–710. https://doi.org/10.1175/JTECH-D-11-00114.1

Heuss, J. M., Fahlbaum, D. F., & Wolff, G. T. (2003). Weekday/weekend ozone differences: What can we learn from them? *Journal of the Air & Waste Management Association*, *53*(7), 772–788. https://doi.org/10.1080/10473289.2003.10466227

Holloway, J. S., Jakoubek, R. O., Parrish, D. D., Gerbig, C., Volz-Thomas, A., Schmitgen, S., et al. (2000). Airborne intercomparison of vacuum ultraviolet fluorescence and tunable diode laser absorption measurements of tropospheric carbon monoxide. *Journal of Geophysical Research*, *105*(D19), 24,251–24,261. https://doi.org/10.1029/2000JD900237

Horie, Y., Cassmassi, J., Lai, L., & Gurtowski, L. (1979). Weekend/weekday differences in oxidants and their precursors, report prepared by Technology Services Corp. for the U.S. Environmental Protection Agency under Contract No. 68–02-2595.

Hu, L., Millet, D. B., Baasandorj, M., Griffis, T. J., Turner, P., Helmig, D., et al. (2015). Isoprene emissions and impacts over an ecological transition region in the U.S. Upper Midwest inferred from tall tower measurements. *Journal of Geophysical Research: Atmospheres*, *120*, 3553–3571. https://doi.org/10.1002/2014JD022732

Huang, M., Bowman, K. W., Carmichael, G. R., Chai, T., Pierce, R. B., Worden, J. R., et al. (2014). Changes in nitrogen oxides emissions in California during 2005–2010 indicated from topdown and bottom-up emission estimates. *Journal of Geophysical Research: Atmospheres*, *119*, 12,928–12,952. https://doi.org/10.1002/2014JD022268

Hutzell, W. T., Luecken, D. J., Appel, K. W., & Carter, W. P. L. (2012). Interpreting predictions from the SAPRC07 mechanism based on regional and continental simulations. *Atmospheric Environment*, *46*, 417–429.

Jacob, D. J., Field, B. D., Li, Q., Blake, D. R., de Gouw, J., Warneke, C., et al. (2005). Global budget of methanol: Constrains from atmospheric observations. *Journal of Geophysical Research*, *110*, D08303. https://doi.org/10.1029/2004JD005172

Jimenez, P. A., & Dudhia, J. (2012). Improving the representation of resolved and unresolved topographic effects on surface wind in the WRF model. *Journal of Applied Meteorology and Climatology*, *51*(2), 300–316. https://doi.org/10.1175/JAMC-D-11-084.1

Kelly, J. T., Baker, K. R., Nowak, J. B., Murphy, J. G., Markovic, M. Z., VandenBoer, T. C., et al. (2014). Fine-scale simulation of ammonium and nitrate over the South Coast Air Basin and San Joaquin Valley of California during CalNex-2010. *Journal of Geophysical Research: Atmospheres*, *119*, 3600–3614. https://doi.org/10.1002/2013JD021290

Kim, S.-W., McDonald, B. C., Baidar, S., Brown, S. S., Dube, B., Ferrare, R. A., et al. (2016). Modeling the weekly cycle of NO_x and CO emissions and their impacts on O3 in the Los Angeles-South Coast Air Basin during the CalNex 2010 field campaign. *Journal of Geophysical Research: Atmospheres*, *121*, 1340–1360. https://doi.org/10.1002/2015JD024292

Kirstine, W., & Galbally, I. E. (2012). The global atmospheric budget of ethanol revisited, atmospheric chemistry and physics. *Atmospheric Chemistry and Physics*, *12*(1), 545–555. https://doi.org/10.5194/acp-12-545-2012

Knote, C., Hodzic, A., Jimenez, J. L., Volkamer, R., Orlando, J. J., Baidar, S., et al. (2014). Simulation of semi-explicit mechanisms of SOA formation from glyoxal in aerosol in a 3-D model. *Atmospheric Chemistry and Physics*, *14*(12), 6213–6239. https://doi.org/10.5194/acp-14-6213-2014

Levitt, S. B., & Chock, D. P. (1976). Weekend-weekday pollutant studies of the Los Angeles basin. *Journal of the Air Pollution Control Association*, *26*, 1091–1092.

Marr, L. C., & Harley, R. A. (2002). Modeling the effect of weekday-weekend differences in motor vehicle emissions on photochemical air pollution in central California. *Environmental Science & Technology*, *36*(19), 4099–4106. https://doi.org/10.1021/es020629x

McDonald, B. C., de Gouw, J. A., Gilman, J. B., Jathar, S. H., Akherati, A., Cappa, C. D., et al. (2018). Volatile chemical products emerging as largest petrochemical source of urban organic emissions. *Science*, *359*(6377), 760–764. https://doi.org/10.1126/science.aaq0524

Millet, D. B., Guenther, A., Siegel, D. A., Nelson, N. B., Singh, H. B., de Gouw, J. A., et al. (2010). Global atmospheric budget of acetaldehyde: 3-D model analysis and constraints from in-situ and satellite observations. *Atmospheric Chemistry and Physics*, *10*(7), 3405–3425. https://doi.org/10.5194/acp-10-3405-2010

Murphy, J. G., Day, D. A., Cleary, P. A., Wooldridge, P., Millet, D. B., Goldstein, A. H., & Cohen, R. C. (2007). The weekend effect within and downwind of Sacramento—Part1: Observations of ozone, nitrogen oxides, and VOC reactivity. *Atmospheric Chemistry and Physics*, *7*(20), 5327–5339. https://doi.org/10.5194/acp-7-5327-2007

Naik, V., Fiore, A. M., Horowitz, L. W., Singh, H. B., Wiedinmyer, C., Guenther, A. A., et al. (2010). Observational constraints on the global atmospheric budget of ethanol. *Atmospheric Chemistry and Physics*, *10*(12), 5361–5370. https://doi.org/10.5194/acp-10-5361-2010

Oetjen, H., Baidar, S., Krotkov, N. A., Lamsal, L. N., Lechner, M., & Volkamer, R. (2013). Airborne MAX-DOAS measurements over California: Testing the NASA OMI tropospheric NO_2 product. *Journal of Geophysical Research: Atmospheres*, *118*, 7400–7413. https://doi.org/10.1002/jgrd.50550

Pollack, I. B., Lerner, B. T., & Ryerson, T. B. (2011). Evaluation of ultraviolet light-emitting diodes for detection of atmospheric NO2 by photolysis-chemiluminescence. *Journal of Atmospheric Chemistry*, *65*(2), 111–125. https://doi.org/10.1007/s10874-011-9184-3

Pollack, I. B., Ryerson, T. B., Trainer, M., Parrish, D. D., Andrews, A. E., Atlas, E. L., et al. (2012). Airborne and ground-based observations of a weekend effect in ozone, precursors, and oxidation products in the California South Coast Air Basin. *Journal of Geophysical Research*, *117*, D00V05. https://doi.org/10.1029/2011JD016772

Qin, Y., Tonnesen, G. S., & Wang, Z. (2004). Weekend/weekday difference of ozone, Ox, CO, VOCs, PM10 and the light scatter during ozone season in Southern California. *Atmospheric Environment*, *38*(19), 3069–3087.

Rappenglück, B., Dasgupta, P. K., Leuchner, M., Li, Q., & Luke, W. (2010). Formaldehyde and its relation to CO, PAN, and SO_2 in the Houston-Galveston airshed. *Atmospheric Chemistry and Physics*, *10*(5), 2413–2424. https://doi.org/10.5194/acp-10-2413-2010

Ryerson, T. B., Andrews, A. E., Angevine, W. M., Bates, T. S., Brock, C. A., Cairns, B., et al. (2013). The 2010 California Research at the Nexus of Air Quality and Climate Change (CalNex) field study. *Journal of Geophysical Research: Atmospheres*, *118*, 5830–5866. https://doi.org/10.1002/jgrd.50331

Ryerson, T. B., Buhr, M. P., Frost, G. J., Goldan, P. D., Holloway, J. S., Hübler, G., et al. (1998). Emissions lifetimes and ozone formation in power plant plumes. *Journal of Geophysical Research*, *103*(D17), 22569–22583. https://doi.org/10.1029/98JD01620

Schauffler, S. M., Atlas, E. L., Blake, D. R., Flocke, F., Lueb, R. A., Lee-Taylor, J. M., et al. (1999). Distributions of brominated organic compounds in the troposphere and lower stratosphere. *Journal of Geophysical Research*, *104*(D17), 21,513–21,535. https://doi.org/10.1029/1999JD900197

Schween, J. H., Hirsikko, A., Lohnert, U., & Crewell, S. (2014). Mixing-layer height retrieval with ceilometer ad Doppler lidar: From case studies to long-term assessment. *Atmospheric Measurement Techniques*, *7*, 3685–3704.

Scott, K. I., & Benjamin, M. T. (2003). Development of a biogenic volatile organic compounds emission inventory for the SCOS97-NARSTO domain. *Atmospheric Environment*, *2*, S39–S49.

Seinfeld, J. H., & Pandis, D. (2006). *Atmospheric chemistry and physics: From air pollution to climate change* (2nd ed.). New York: John Wiley.

Singh, H., Chen, Y., Tabazadeh, A., Fukui, Y., Bey, I., Yantosca, R., et al. (2000). Distribution and fate of selected oxygenated organic species in the troposphere and lower stratosphere over the Atlantic. *Journal of Geophysical Research*, *105*(D3), 3795–3805. https://doi.org/10.1029/1999JD900779

Singh, H. B., Salas, L., Chatfield, R., Czech, E., Fried, A., Walega, J., et al. (2004). Analysis of the atmospheric distribution, sources, and sinks of oxygenated volatile organic chemicals based on measurements of the Pacific during TRACE-P. *Journal of Geophysical Research*, *109*, D15S07. https://doi.org/10.1029/2003JD003883

Skamarock, W. C., Klemp, J. B., Dudhia, J., Gill, D. O., Barer, D. M., Duda, M., et al. (2008). A description of the advanced research WRF version 3., NCAR Technical Note.

Stephens, S., Madronich, S., Wu, F., Olson, J. B., Ramos, R., Retama, A., & Munoz, R. (2008). Weekly patterns of México City's surface concentrations of CO, NO_x, PM_{10} and O_3 during 1986–2007. *Atmospheric Chemistry and Physics*, *8*(17), 5313–5325. https://doi.org/10.5194/acp-8-5313-2008

Träumner, K., Kottmeier, C., Corsmeier, U., & Wieser, A. (2011). Convective boundary-layer entrainment: Short review and progress using Doppler lidar. *Boundary-Layer Meteorology*, *141*(3), 369–391. https://doi.org/10.1007/s10546-011-9657-6

United States Environmental Protection Agency (2018). Modeling guidance for demonstrating air quality goals for ozone, PM2.5, and regional haze. Retrieved from https://www.epa.gov/scram/state-implementation-plan-sip-attainment-demonstration-guidance

Wagner, N. L., Dubé, W. P., Washenfelder, R. A., Young, C. J., Pollack, I. B., Ryerson, T. B., & Brown, S. S. (2011). Diode laser-based cavity ring-down instrument for NO_3, N_2O_5, NO, NO_2 and O_3 from aircraft. *Atmospheric Measurement Techniques*, *4*(6), 1227–1240. https://doi.org/10.5194/amt-4-1227-2011

Warneke, C., de Gouw, J. A., Edwards, P. M., Holloway, J. S., Gilman, J. B., Kuster, W. C., et al. (2013). Photochemical aging of volatile organic compounds in the Los Angeles basin: Weekday-weekend effect. *Journal of Geophysical Research: Atmospheres*, *118*, 5018–5028. https://doi.org/10.1002/jgrd.50423

Warneke, C., McKeen, S. A., de Gouw, J. A., Goldan, P. D., Kuster, W. C., Holloway, J. S., et al. (2007). Determination of urban volatile organic compound emission ratios and comparison with an emissions database. *Journal of Geophysical Research*, *112*, D10S47. https://doi.org/10.1029/2006JD007930

Woody, M. C., Baker, K. R., Hayes, P. L., Jimenez, J. L., Koo, B., & Pye, H. O. T. (2016). Understanding sources of organic aerosol during CalNex-2010 using CMAQ-VBS. *Atmospheric Chemistry and Physics*, *16*(6), 4081–4100. https://doi.org/10.5194/acp-16-4081-2016

Yarwood, G., Stoeckenius, T. E., Heiken, J. G., & Dunker, A. M. (2003). Modeling weekday/weekend ozone differences in the Los Angeles region for 1997. *Journal of the Air & Waste Management Association*, *53*(7), 864–875. https://doi.org/10.1080/10473289.2003.10466232